Summer 8-15-2015

Programming the Myocardium: the Notch-Wnt Axis

Benjamin S. Gillers
Washington University in St. Louis

WASHINGTON UNIVERSITY IN ST. LOUIS
Division of Biology and Biomedical Sciences
Developmental, Regenerative, and Stem Cell Biology

Dissertation Examination Committee:
Stacey Rentschler, Chair
Donald Elbert
Robert Mecham
Jeanne Nerbonne
David Ornitz
Jim Skeath

Programming the Myocardium: the Notch-Wnt Axis

by
Benjamin Saul Gillers

A dissertation presented to the
Graduate School of Arts & Sciences
of Washington University in
partial fulfillment of the
requirements for the degree
of Doctor of Philosophy

August 2015
St. Louis, Missouri

Table of Contents

List of Figures

List of Abbreviations

AC arrhythmogenic cardiomyopathy

AVC atrioventricular canal

AVN atrioventricular node

AVJ atrioventricular junction

BLI bioluminescence imaging

ID intercalated disc

NICD Notch intracellular domain

Acknowledgements

I thank Dr. Ben Stanger for providing *tetO-NICD* mice and Dr. Konrad Basler for providing *DM* mice. I would like to acknowledge Stephanie Hicks, Dr. Baas Boukens, Dr. Haytham Aly, Dr. Aditi Chiplunkar, Chaoyi Kang, Jon Qiao, and Kailin Baechle for their experimental contributions. Their individual contributions are listed at the end of each chapter. I would also like to thank Dr. Attila Kovacs and Carla Weinheimer of the Mouse Cardiovascular Phenotyping Core in the Center for Cardiovascular Research for performing echocardiograms and gene painting thoracotomies, Julie Prior and the Optical Radiology Lab for BLI, and Bill Coleman and Marlene Scott of the Developmental Biology Histology & Microscopy Core at Washington University for invaluable technical assistance and guidance. I would like to thank Dr. Michal Pasque, the Midwest Transplant Services, and the families of heart donors for their help and contributions. This work was supported by the American Heart Association and Ms. Pamela Marks (predoctoral fellowship 12PRE8570003). I would like to thank Dr. Igor Efimov and his entire lab for their fantastic collaboration. Thank you to Dr. David Curiel and Dr. Igor Dmitriev for their collaboration and viruses. I would like to thank my committee chair, Dr. Jim Skeath and my entire committee, Dr. Jeanne Nerbonne, Dr. David Ornitz, Dr. Robert Mecham, and Dr. Donald Elbert for their invaluable guidance and mentorship. I would like to thank my advisor, Dr. Stacey Rentschler for her fantastic teachings and support and the awesome opportunity to do my thesis research in her lab.

ABSTRACT OF THE DISSERTATION

Programming the Myocardium: the Notch-Wnt Axis

by

Ben Gillers

Doctor of Philosophy in Biology and Biomedical Sciences

Developmental, Regenerative, and Stem Cell Biology

Washington University in St. Louis, 2015

Professor Stacey Rentschler, Chair

Heart related deaths are the number one cause of death in the United States. While heart failure and other mechanical issues are common, arrhythmias account for the majority of these deaths. By understanding the genetic architecture that patterns the normal cardiac conduction system, we can further deepen our understanding of how arrhythmias arise and develop targeted therapies to treat this deadly class of disease. I have found that canonical Wnt signaling is necessary for development of the atrioventricular junction. Furthermore, absence of myocardial Wnt signaling leads to tricuspid atresia. Overexpression of Wnt signaling leads to development of ectopic atrioventricular junction tissue and induces delayed conduction velocity and other electrophysiological properties of nodal tissue. I have further found that Wnt signaling is downregulated by Notch signaling and this downregulation is required for Notch induced ventricular preexcitation. I have also developed a gene therapy platform for testing the role of these genes in cultured mouse and human cardiac tissue.

Chapter 1: Introduction

1.1 The Cardiac Conduction System

The mammalian heart is comprised of four chambers: the right and left atria and ventricles. Their function is to pump blood throughout the body through sequential atrial and ventricular contraction. This contraction is regulated by the cardiac conduction system; a network of electrically active, specialized cardiomyocytes which control myocyte activation[1]. The electrical impulse originates in the sinoatrial node (SAN), situated in the right atrium (RA) between the superior and inferior vena cava. The impulse travels to the atrioventricular node (AVN) where the conduction velocity is decreased. This allows sequential atrial and then ventricular activation and contraction; thereby allowing atrial to ventricular blood flow. Crucial to this function is the atrioventricular junction (AVJ) in the adult heart and its embryonic precursor, the atrioventricular canal (AVC). The AVJ is composed of slow conducting myocardial tissue and the annulus fibrosis, an insulating plane of fibroblasts and adipocytes[2]. The annulus prevents any electrical conduction between atria and ventricles except through the slow conducting AVN. In the embryo, where the annulus is not yet formed, this electrical segregation is achieved through the slow conducting nature of the AVC myocardium [3].

Cardiac conduction can be measured using the electrocardiogram (ECG). Leads are placed in different regions of the body and can measure numerous electrical properties of the heart including atrial activation (P wave), ventricular activation (QRS complex), and the time between atrial and ventricular activation (PR Interval) [4].

The AVC is programmed through an integrated network of transcription factors and other genes. The Tbox family of transcription factors, is perhaps the most important group of genes in AVC development. Loss of Tbx2, Tbx3, or Tbx20 all have deleterious effects on AVC development. Furthermore, the expression of these three genes is primarily limited to the AVC region, albeit in partially overlapping patterns. While Tbx2 and 3 are expressed only in myocytes, Tbx20 is expressed in AVC myocytes and non-myocytes. In addition to the Tbox factors, Bmp2 singling is required for AVC development and, likewise, its cardiac expression is primarily limited to the AVC region[5-12].

Wolff-Parkinson-White (WPW) syndrome is an important disease involving the AVJ. This disease is characterized by development of accessory pathways- fast conducting myocardial tissue which electrically connect the atria and ventricles. In addition there is loss of the annulus fibrosis. Most importantly, there is a reduction in the PR interval and appearance of the delta wave on the ECG. The patient may feel palpitations which require follow up with an ECG [13, 14]. Several mouse models of this disease have been developed including manipulation of *Tbx2*, *Tbx3* and most recently, Notch signaling [15-18]. By overexpressing Notch signaling in a subset of ventricular myocardium, accessory pathways develop, there is a dramatic PR interval shortening, and the annulus does not develop. Of note, this phenotype is 100% penetrant. The mechanism of Notch induced ventricular preexcitation will be discussed in greater detail in chapter 4.

When dissecting genetic pathways in mice, many different Cre drivers are available to induce recombination in myocytes. The $Mlc2v^{Cre}$ is a knock in allele in the *Mlc2v* locus. Importantly, while this Cre is activated early in development, it is only expressed in a subset of ventricular

myocytes. This Cre is particularly useful when perturbation of the gene of interest is embryonic lethal if recombined in all myocytes. The spotty expression of the *Mlc2v*^{Cre} allows mice with deleterious phenotypes to survive to adulthood. However, since it is only expressed in a subset of myocytes, its utility in gene expression studies is limited [19]. Another common Cre is the *αMHC-Cre*, a transgenic allele in which Cre is expressed under the regulation of the *αMHC* transgene. Although expressed later in development than the *Mlc2v*^{Cre}, this Cre is expressed in almost all cardiac myocytes [20]. This allele is particularly useful for gene expression studies. Lastly, the *Tbx2*^{Cre} is another usefult tool. This Cre, a knockin allele, is expressed in Tbx2 + myocytes. At e9.0, this is expressed only in AVC myocytes [11].

1.2 Wnt Signaling

Wnt signaling is one of the most pervasive signaling pathways in development and disease. This pathway is composed of numerous ligands which can bind a member of the Frizzled family of cell surface receptors. Frizzled, in turn, is bound to Dishevelled protein. There are two classes of Wnt signaling: non-canonical and canonical. Non-canonical Wnt singling is independent of β-catenin and canonical Wnt signaling is dependent on β-catenin. There are two sub-categories of non-canonical Wnt signaling: the planar cell polarity pathway and the calcium handling pathway [21-23]. Canonical Wnt signaling is the focus of this dissertation and I will focus on it here.

As mentioned, canonical Wnt signaling is β-catenin dependent. Normally β-catenin is translated in the cytoplasm and is targeted for degradation by the degradation complex, composed of Axin, PP2A, APC, and GSK3β. GSK3β phosphorylates β-catenin on 5 serine and threonine residues in exon 3 which signals for it to be degraded by the lysosome. This prevents accumulation of β-

catenin in the cytoplasm. When a Wnt ligand reaches the cell surface, it binds the Frizzeled receptor, a member of the G protein Coupled Receptor family, and its co-receptor, Lrp5/6. Dishevelled, bound normally by Frizzled than causes translocation of the degradation complex to the plasma membrane. Upon this translocation, it can no longer function to target β-catenin for degradation. Once β-catenin accumulates in the cytoplasm it localizes to the nucleus. Once there, it binds one of the TCF or LEF proteins that is bound to target DNA sequences. Upon binding, downstream transcription is initiated [24, 25].

One of the most reliable direct targets of canonical Wnt signaling is *Axin2* which acts as a negative regulator of canonical Wnt signaling. $Axin2^{LacZ}$ constructs are used in cell culture and mice as a readout of active canonical Wnt signaling[26].

Canonical Wnt signaling was first discovered as a protoc-oncogene but has since been shown to regulate a host of developmental processes in every model organism studied such as cellular proliferation, cell fate specification, epithelial to mesenchymal transition (EMT), and mitochondrial biogenesis [22, 27-29].

An important point to keep in mind when studying canonical Wnt signaling is the dual role of β-catenin. While this protein lies at the nexus of this pathway, it also plays a fundamental role in cellular adhesion. β-catenin can be localized in the cytoplasm from where it translocates to the nucleus. However, β-catenin is also localized to the cell membrane where it stabilizes cadherins and thereby promotes cell-cell adhesion. In the absence of β-catenin, cadherins lack structural integrity and cadherins from neighboring cells do not bind each other. In myocytes, membrane β-

catenin is primarily localized to the intercalated discs (ID) which lie at the myocyte-myocyte junction. It is co-localized with other important ID proteins such as N-cadherin, plakogoloin, and plakophillin. Integrity of the ID is crucial for normal development. Mutations in a number of ID genes result in arrhythmogenic cardiomyopathy (AC), a disease characterized by fibrottay deposition and an arrhythmia prone heart [30, 31]. It has been posited, based on zebrafish models of AC, that loss of Wnt signaling may lead to AC [30]. This hypothesis will be challenged in chapter 3 of this dissertation.

Because of the dual role of *β-catenin*, when over expressing or knocking out this gene, one needs to carefully dissect which role of *β-catenin* is important. A specific signaling allele of *β-catenin* was developed by Konrad Bassler's lab in which only its signaling role but not cell adhesion role is perturbed. This is achieved by point mutations in the N and C termini while leaving the rest of the protein functional [32]. I use this allele in my LOF studies in chapter 2 to specifically dissect the role Wnt signaling in AVC develpment. However, in the gain of function studies, in which exon 3 is deleted, one must be careful in interpretation of the results since not only is one increasing Wnt signaling but also potentially affecting cell adhesion.

Wnt signaling plays many important roles in cardiac development including regulating cell specification and proliferation [23, 33-35]. Recently, using a global knockout of the Wnt ligand, Wnt2, Tian et al have shown that loss of Wnt signaling leads to loss of the AVC [36]. However, since that study used a global knockout, it remains unclear which cell type requires Wnt signaling. Is it the myocytes, endothelial cells, fibroblasts or other cell types? Using a myocyte specific model of Wnt LOF, I will address this question in chapter 2 of this dissertation.

1.3 Notch Signaling

Notch signaling is another fundamental signaling pathway involved in development and disease. It has one of the longest histories in developmental biology, as its first allele was discovered in drosophila by the famous Thomas Hunt Morgan in 1917 [37]. While the Wnt singling cascade is initiated by a secreted ligand, Notch signaling is initiated by a cell surface ligand binding to a receptor of an adjacent cell. Because of this property, Notch signaling is famous for establishing boundaries between different cell and tissue types because the cells expressing the ligand can induce a specific fate on neighboring cells that contain the receptor. For example, hair stem cells are known to express the Notch Ligand whereas neighboring cells which express the receptor are then specified and differentiate [38].

The Notch signaling cascade is activated by one of two transmembrane ligand families, delta-like and jagged. The signal receiving cell expresses one of four receptors, Notch1-4. Upon ligand binding to the receptor, the Notch IntraCellular Domain (NICD) is released due to cleavage of the receptor by an adam family mellaprotease. Gama secretase then cleaves the actual NICD and releases it for nuclear translocation. Once in the nucleus, NICD binds and activates the CSL transcription factor which activates downstream transcription [39].

Notch signaling has long been known to play a role in multiple cancers. Many anti-Notch therapies have been developed and many have failed in clinical trials due to their negative side effects on the cardiovascular system [40]. This highlights the importance of Notch signaling in this area. Because the heart is such a complex tissue with many regional differences, Notch signaling

is crucial to understanding its development. In fact, Notch signaling has long been known to be involved in cardiac development. The direct Notch targets, Hey1 and Hey2 are required for limiting *Bmp2* and *Tbx2* expression to the AVC. This is because Notch activity in the atria and ventricles inhibits *Bmp2* and *Tbx2* in those tissues [41, 42]. Why Notch is not active in the AVC remains an important and open question.

Because of the importance of Notch signaling in the cardiovascular system, our lab has previously tested the effect of cardiac Notch activation. Overexpression of NICD using the $Mlc2v^{Cre}$ causes formation of accessory pathways connecting the RA and RV; similar to those seen in WPW patients. Furthermore, the annulus fibrosis and AV groove are lost and these mice develop a shortened PR interval, also characteristic of WPW patients [18]. This study highlights the importance of regional activation of Notch signaling. When that regionality is breached, the specific identity of the AVJ is perturbed. The mechanism of Notch induced ventricular preexcitation and the involvement of Wnt signaling in this phenotype will be explored in chapter 4.

1.4 Cardiac Gene Therapy

Gene therapy presents an important method for using Notch and Wnt signaling for therapeutic purposes. However promising, it has seen a long and bumpy bumpy road. In the late 1990s, it was presented as the next big thing in targeted therapies. However, due to the death of Jesse Gelsinger, a 19 year old who died due to complications in a gene therapy clinical trial, the field has been set back over a decade[43]. However, since the death of Gelsinger, a great deal has been learned about the challenges and risks of gene therapy and scientists have been perfecting this

technology ever since. As momentum for gene therapy gains, it is prime time to reinvest our efforts in this technology.

Gene therapy, broadly defined, involves the delivery of exogenous genes to either correct a mutation in the patient or to overexpress a specific isoform of the gene(s) of interest [44]. Mutational correction has been demonstrated in mice, as proof of principle, to treat sickle cell anemia [45]. However, due to the difficulty in correcting mutations in adult cells that have low proliferative rates, gene therapy as an overexpression platform provides a much broader scope for potential therapies.

Any form of delivery of genetic material can be used to this end. However, delivery of the coding sequence without some form of a carrier is highly inefficient in uptake into target cells. For this reason, viruses have been used as promising vectors. They are highly efficient at delivering DNA to the tissue of interest and can be modified to target specific cell types [44].

The 3 main types of virus used in gene therapy are 1) lentivirus, 2) adenovirus and 3) adeno-associated virus (AAV). The benefit of lentivirus is that it integrates within the host genome. Therefore, it can be used to correct host mutations and can be used for stable, permanent overexpression. However, therein also lies its greatest risk. Because it can insert into the genome, it has the potential of inserting into oncogenes or other sites that can have drastic side effects [44].

For example, in a clinical trial at the turn of this millennium to treat X-linked severe combined immunodeficiency, one of the subjects developed T-cell leukemia due to the insertion site of the

gene of interest. In this particular case, the patient presented with symptoms only 2 ½ years after enrollment in the trial making long term follow-up absolutely imperative and proving safety here to be a daunting task [46].

Because of this risk, for overexpression platforms, adenovirus or AAV are preferred. The benefit of adenovirus over AAV is that it can contain a larger insert. This is particularly important for multigenic constructs. However, they have the property of inducing an immune response and therefore, cells infected with the virus, can be cleared by the immune system, thereby defeating the goal of therapy. For this reason, AAV may be preferred over adenovirus by some [47]. However, current technologies exist to prevent immune system activation by adenovirus [48].

While the majority of viral based gene therapy clinical trials have taken place in the cancer space, there is a great deal of effort to use them for cardiovascular disease [44]. The field faces several challenges; for example, localized delivery of the gene of interest. One can imagine that overexpression of a gene could be beneficial to one chamber of the heart while deleterious to the rest of it. For example, one of the biggest challenges in atrial fibrillation drugs remains the negative side effects of the drug on parts of the heart other than its target tissue [49]. For this reason, viral injection in the blood stream is limited in its utility. One way to solve this problem is by developing specific targeting molecules on the viral capsid surface which would allow the viral particle to home in on a certain tissue or certain cell type, thereby limiting its negative side effects. An alterative to this method is localized injection, either catheter or surgery based. When developing one of these approaches, one needs to take into consideration the risks and ease of delivery for this procedure and balance it to the benefit of that particular therapy.

In this dissertation, I will first discuss the role of canonical Wnt signaling in AVC development and disease. I will then discuss how Wnt signaling is regulated by Notch signaling. Lastly, I will discuss the development of novel tools for the use in gene therapy studies.

Chapter 2: Canonical Wnt is Required for AVC Development

2.1 Canonical Wnt Signaling is Active in the Developing AVC

To first ascertain whether it is likely for canonical Wnt signaling to be involved in development of the AVC, I assayed the temporal and spatial distribution of active Wnt signaling in the murine heart. To assay this, I used the *Axin2*^{LacZ} mouse. *Axin2* is a direct transcriptional target of canonical Wnt signaling. The role of *Axin2* is to serve as a negative feedback loop and limit the activity of Wnt singling once activated. In this mouse, *LacZ* is knocked into the *Axin2* promoter. Therefore, β galactosidase activity indicates where *Axin2* is expressed and where Wnt signaling is active.

I performed a timecourse of *LacZ* expression from E10.5 to E17.5 and analyzed both whole mount hearts and histological sections. Starting at E10.5, *Axin2*^{LacZ} is most strongly expressed in the AVC. Through E17.5, the AVC remains the primary region of *Axin2*^{LacZ} expression. As can been seen at E17.5, *Axin2*^{LacZ} is expressed both in the AVC myocardium and valve tissue; leading to the possibility that canonical Wnt signaling plays a role in both tissue types (figure 1).

Outside of the AVC, there is sporadic expression in both atria and ventricles. Interestingly, there is significant expression in the SAN region (and SVC valve leaflets) (figure 1G,H). This leads to the intriguing possibility that Wnt signaling may also play a role in sinus node development.

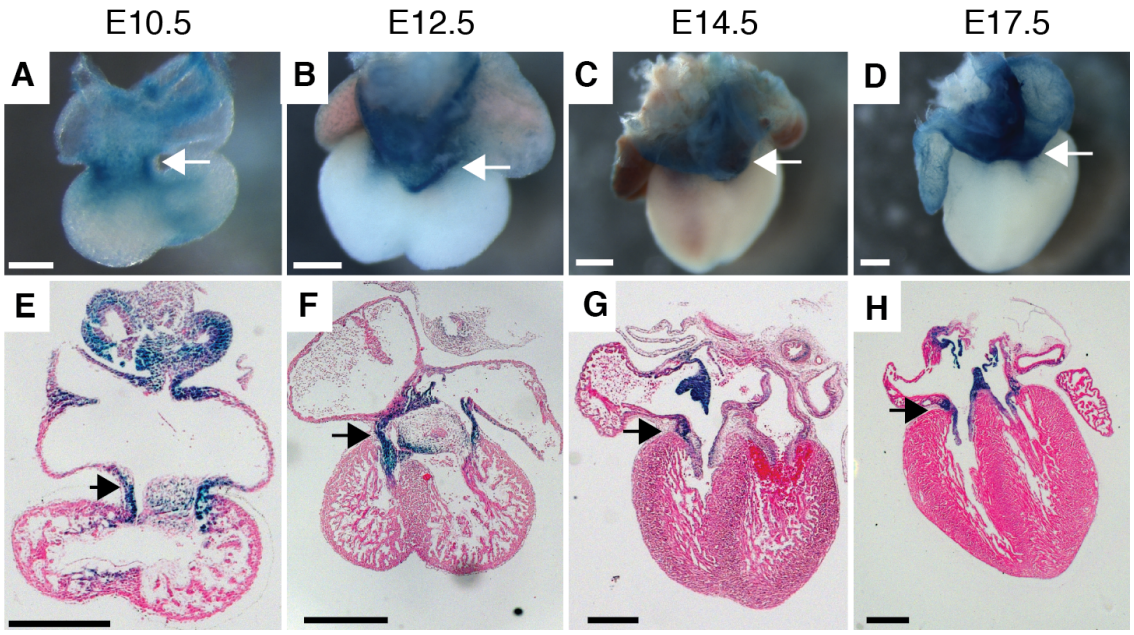

Figure 1. Canonical Wnt signaling is active in the developing AVC
(A-D) Developmental timecourse of *Axin2*^{LacZ} expression as assessed by Xgal staining denotes active canonical Wnt signaling in the region of the AV canal in hearts imaged from the posterior view (white arrows). (E-H) Histological sections of hearts from panels A-D reveal *Axin2*^{LacZ} expression within AV canal myocardium (black arrows). Scale bars 500 μm.

2.2 Loss of Myocardial Canonical Wnt Signaling Results in Tricuspid Atresia

To test the role of canonical Wnt signaling in the myocardium, 2 separate alleles of *β-catenin* were used. The first allele is a conditional deletion of *β-catenin*. In cells that express Cre recombinase, this allele of *β-catenin* is deleted. The second allele is the Double Mutant (DM) allele in which there are point mutations in the N and C termini of *β-catenin* thereby turn off the signaling role of β-catenin [32]. However, the main body of the protein is not perturbed, thereby leaving the cell adhesion role of β-catenin intact. When these two alleles are combined with the *αMHC-Cre*, a myocyte specific Cre, all non-myocytes are heterozygous for the DM allele and WT for the conditional allele. However, myocytes in which Cre is expressed loose their conditional allele. This allowed me to test the signaling role of β-catenin specifically in cardiomyocytes.

Hearts in Wnt LOF mice appeared normal at E10.5. Both the gross morphology and AVC histology had no detectable differences between control and mutant mice. However, at E18.5 Wnt LOF displayed tricuspid atresia, RV hypoplasia, and loss of the AVC (figure 2). At E10.5, the heart valves are not yet developed and exist in their precursor form, the AV cushions [50]. This group of mesenchymal cells sits in the common canal region, connecting the atria and ventricles. No abnormal morphology exists in the cushions. By E14.5, after the cushions have undergone EMT, the early valves are condensed and formed. The valve precursors develop in Wnt LOF, although their morphology is slightly abnormal (figure 2C,G,K,O). At this time, there is clear continuity between the RV and RA, through the tricuspid valve precursor, in both control and Wnt LOF. However, by E18.5, no continuity can be seen between the RV and RA and the tricuspid valve is completely absent (figure 2D,H,L,P).

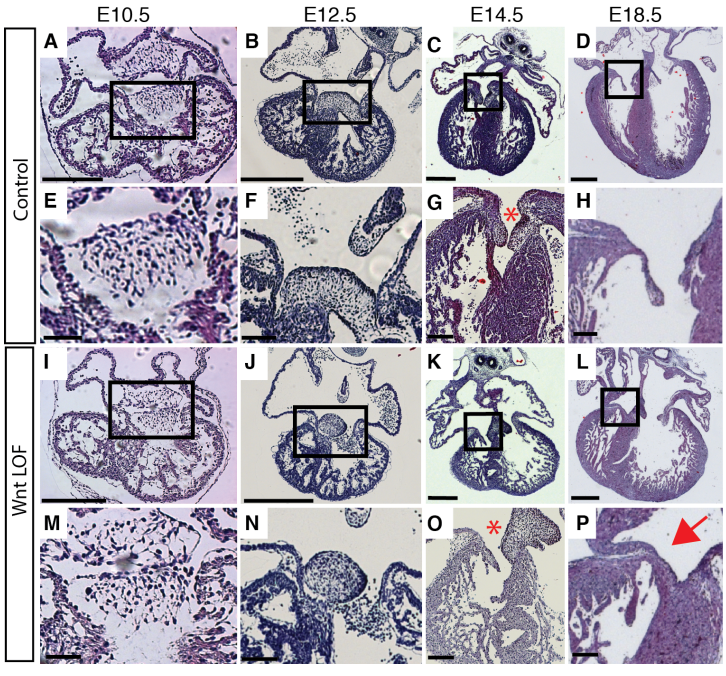

Figure 2. Loss of myocardial canonical Wnt signaling results in congenital heart defects. Trichrome staining of representative sections from *αMHC-Cre; Ctnnb1*$^{dm/fl}$ (Wnt LOF) mice show normal development at E10.5 (A,E,I,M) and E12.5 (B,F,J,N) when compared with littermate controls. By E14.5, the tricuspid valve is under-developed and the right ventricle is hypoplastic in Wnt LOF mice (C,G,K,O). The red asterisks denotes a similar size opening between right atrium and right ventricle in control and Wnt LOF mice (O,W), while a hypoplastic right heart can already be seen in Wnt LOF embryos. By E18.5, the tricuspid valve is completely absent in Wnt LOF mice (D,H,L,P). The red arrow in P denotes the region of the atretic valve. Panels E-H are higher magnification images from boxed regions in A-D, respectively. Panels M-P are higher magnification images from boxed regions in I-L, respectively. Scale bars 500 μm in A-D, I-L and Q-T. Scale bars 125 μm in E-H and M-P.

This phenotype was observed only when

deleting *β-catenin* with the *αMHC-Cre*. However, when using the $Mlc2v^{Cre}$, the tricuspid valve develops normally. Cd31 expression, which marks endocardial tissue and therefore outlines the valve, appears normal when using the $Mlc2v^{Cre}$, further highlighting the lack of a phenotype with this Cre (figure 3). This is most likely explained based on the different expression of these 2 Cre drivers. The $Mlc2v^{Cre}$ is expressed only in a subset of ventricular myocardium whereas the *αMHC-Cre* is expressed in almost all myocytes (figure 4). This difference is particularly striking when observing the AVC myocardium.

The development of tricuspid atresia is particularly noteworthy since I deleted Wnt signaling with a myocyte specific Cre and yet the tricuspid valve, not myocardial in origin, was severely affected. There are several hypotheses that could explain this. First, myocyte Wnt signaling could induce a downstream non-cell autonomous signal that is required for development of the valves. Alternatively, the AVC myocardium is required to serve as a migration substrate of the developing valves. In the absence of that tissue, the condensing cushions die. As will be discussed, the AVC myocardium is lost in Wnt LOF mice which may therefore affect valve maturation and survival.

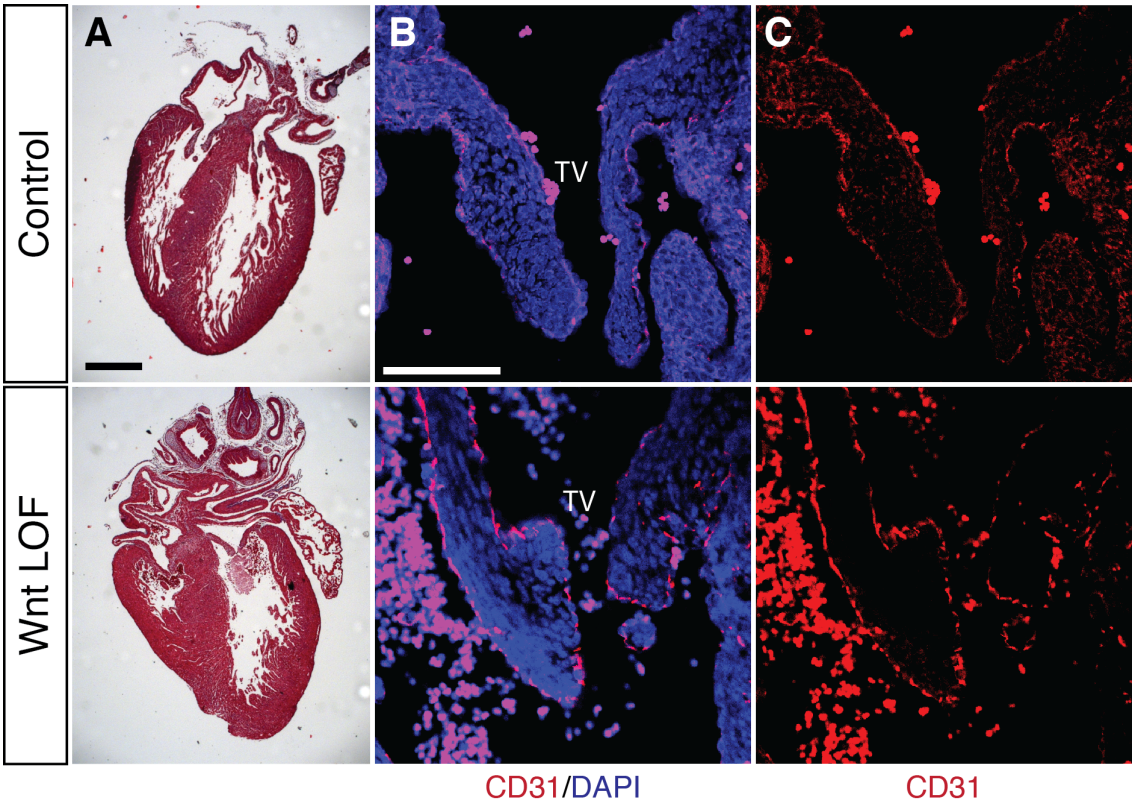

Figure 3. Complete loss of β-catenin within the ventricles leads to abnormal right ventricular development with normal tricuspid valve formation.
Trichrome staining at E16.5 shows a malformed RV in *Mlc2v*$^{Cre/+}$*;Ctnnb1*$^{fl/fl}$ when compared with control (A) and IHC staining for CD31 delineates grossly normal tricuspid valve morphology in *Mlc2v*$^{Cre/+}$*;Ctnnb1*$^{fl/fl}$ when compared with control (B,C). Scale bar in A is 500 μm. Scale bar in B corresponds to B,C and is 100 μm.

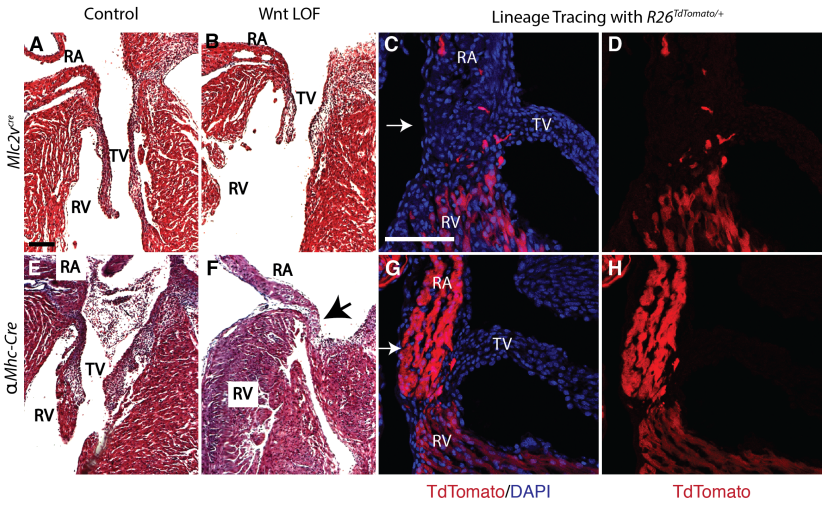

Figure 4. Deletion of *β-catenin* within the AVJ myocardium leads to tricuspid valve defects.
(A,B) In *Mlc2v*$^{Cre/+}$*; Ctnnb1*$^{dm/fl}$ the tricuspid valve (B) is grossly similar to that in control (A) as assessed by Trichrome staining. Lineage tracing analysis demonstrates that *Mlc2v*^{Cre} is expressed in a subset of ventricular myocytes, while only very sparsley within the AV junction as assessed in *Mlc2v*$^{Cre/+}$*; R26*$^{TdTomato/+}$ hearts (C,D). (E-H) In *αMHC-Cre; Ctnnb1*$^{dm/fl}$ mice where recombination occurs throughout the entire AV junction (G,H), the tricuspid valve is atretic (F compared to E). Black arrow in F denotes region of atretic tricuspid valve. White arrows in C, G denote the AV junction. Scale bar in A corresponds to A,B,E,F, scale bar in C corresponds to C,D,G,H and both are 100 μm.

In the absence of a tricuspid valve I hypothesized that blood flow would predominately occur between the LA and LV while no blood flow would occur between the RA and RV. This is because in place of a valve between the RA and RV, there is myocardium and no opening between the chambers through which blood can flow. To test this hypothesis, echocardiography was used to measure blood flow. Indeed, robust blood flow is seen between the LA and LV while almost no flow is seen between the RA and RV. The little flow that is seen may be through a small continuity connecting the RA and RV; however, normal flow, as seen in the left side of the heart, is abrogated (figure 5).

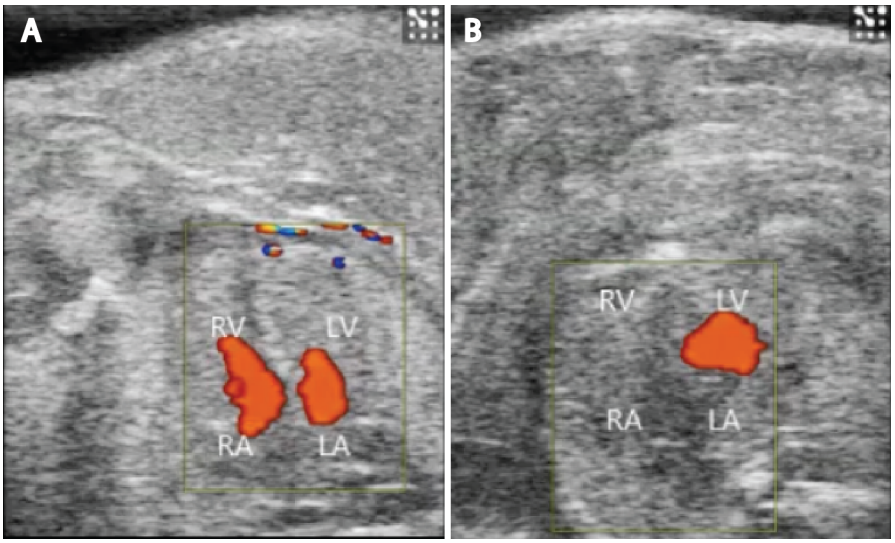

Figure 5. RA to RV blood flow is abrogated in Wnt LOF hearts
Freeze frames of echocardiographs of embryonic hearts at E18.5 In control (A) blood flow is seen from the LA to LV and RA to RV (orange). In Wnt LOF hearts (B), blood flow is seen only from the LA to LV but not RA to RV.

Another important morphological phenotype is the development of septal defects. Both severe membranous and muscular ventricular septal defects were highly penetrant in Wnt LOF mice (figure 6). Furthermore, these mice display severe RV hypoplasia (figure 6). While the membranous septal defects may be mechanistically related to the AVC defects, the muscular septal defects and the hypoplastic RV likely suggest a separate role for Wnt signaling in those

tissues. Since Wnt activity is low outside of the AVC at the assayed timepoints, these defects are either suggestive of a very high sensitivity to Wnt dosing or perhaps the result of an earlier Wnt requirement in those tissues.

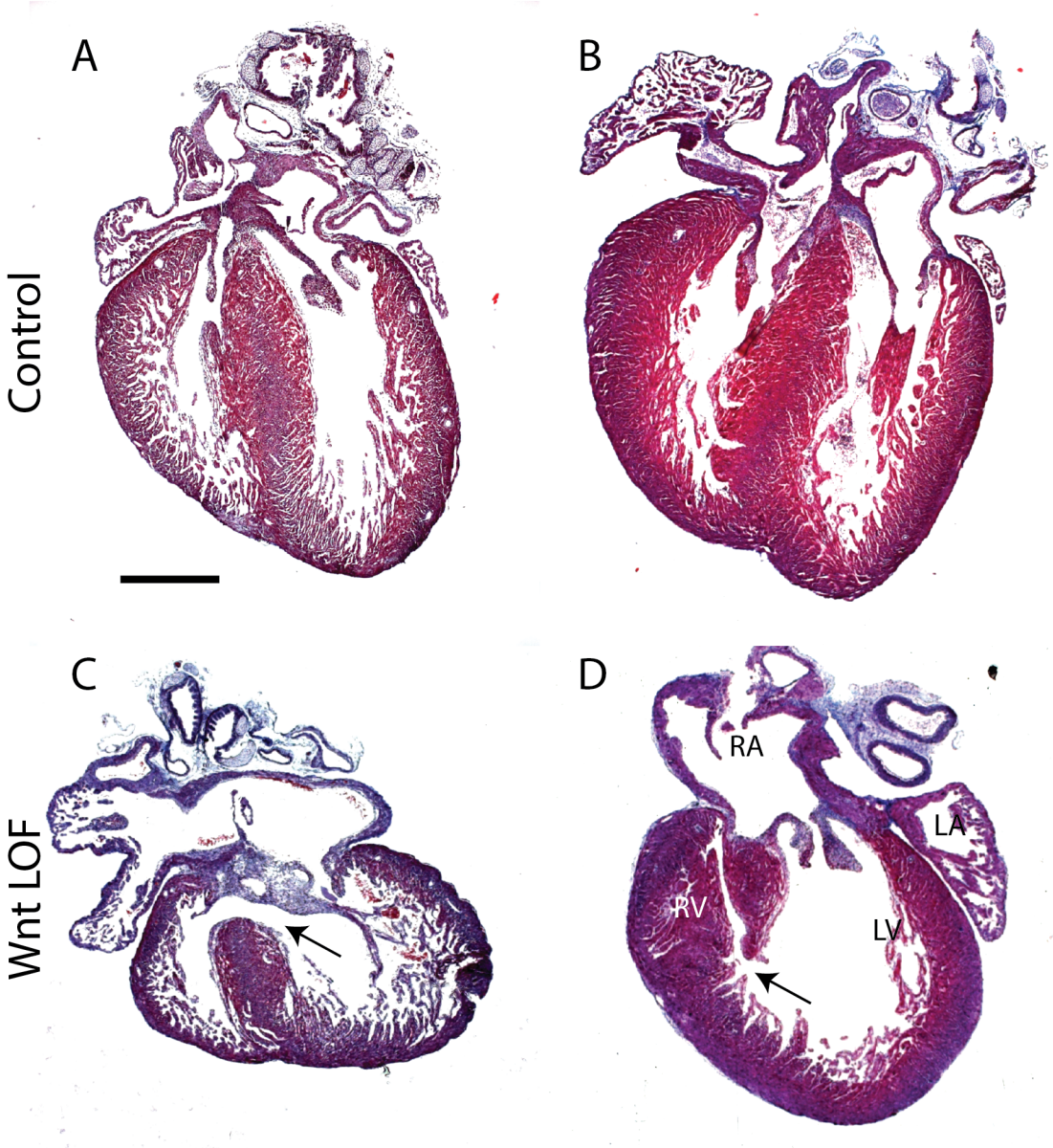

Figure 6. Wnt LOF mice exhibit septal defects.
Trichrome staining of *αMHC-Cre; Ctnnb1*$^{dm/fl}$ demonstrates prominent septal defects at E17.5 (C) and P0 (D) when compared with littermate controls (A and B respectively). Panel C demonstrates a membranous ventricular septal defect, while panel D demonstrates a muscular ventricular septal defect. Scale bar corresponds to A-D and is 500 μm.

2.3 Loss of Myocardial Canonical Wnt Signaling Results in Loss of AVC Myocardium

Since canonical Wnt signaling is active in the AVC myocardium, I wanted to determine if the AVC myocardium was affected by loss of Wnt signaling. The AVC contains a specific expression pattern. AVC myocytes express Tbx2, 3 and Bmp2 [6, 10, 51, 52]. Non-moycytes in the AV canal express periostin in a spider web-like network around the Tbx3 positive myocytes [53, 54]. Furthermore, while working myocardium myocytes express high conductance gap junction proteins (Connexin 43 (Cx43) in the ventricle and Connexin 40 (Cx40) in the atria), the AVC myocardium does not [55, 56].

I assayed these markers in the Wnt LOF mice. There is a dramatic absence of Tbx3/periostin staining in the plane of the annulus in Wnt LOF mice. In addition, in serial sections, there is a reduction in the Cx40 + tissue in this region. Furthermore, using in situ hybridization, I detected a substantial reduction in *Bmp2* + tissue in the plane of the annulus (figure 7).

Combined, these data suggest that canonical Wnt signaling is not only expressed in the developing AVC but is required for its maturation. In these experiments, the *αMHC-Cre* was used to induce recombination of the *β-catenin* allele. While there is an absence of AVC markers by e18.5, AVC development appears normal at E10.5. Both gross histology and AVC markers do not appear perturbed at this stage (figure 2I,M and data not shown). This suggests that canonical Wnt signaling is actively required for continual development of the AVC. Although the canal is present at e10.5, upon loss of canonical Wnt signaling, this tissue is lost by E18.5.

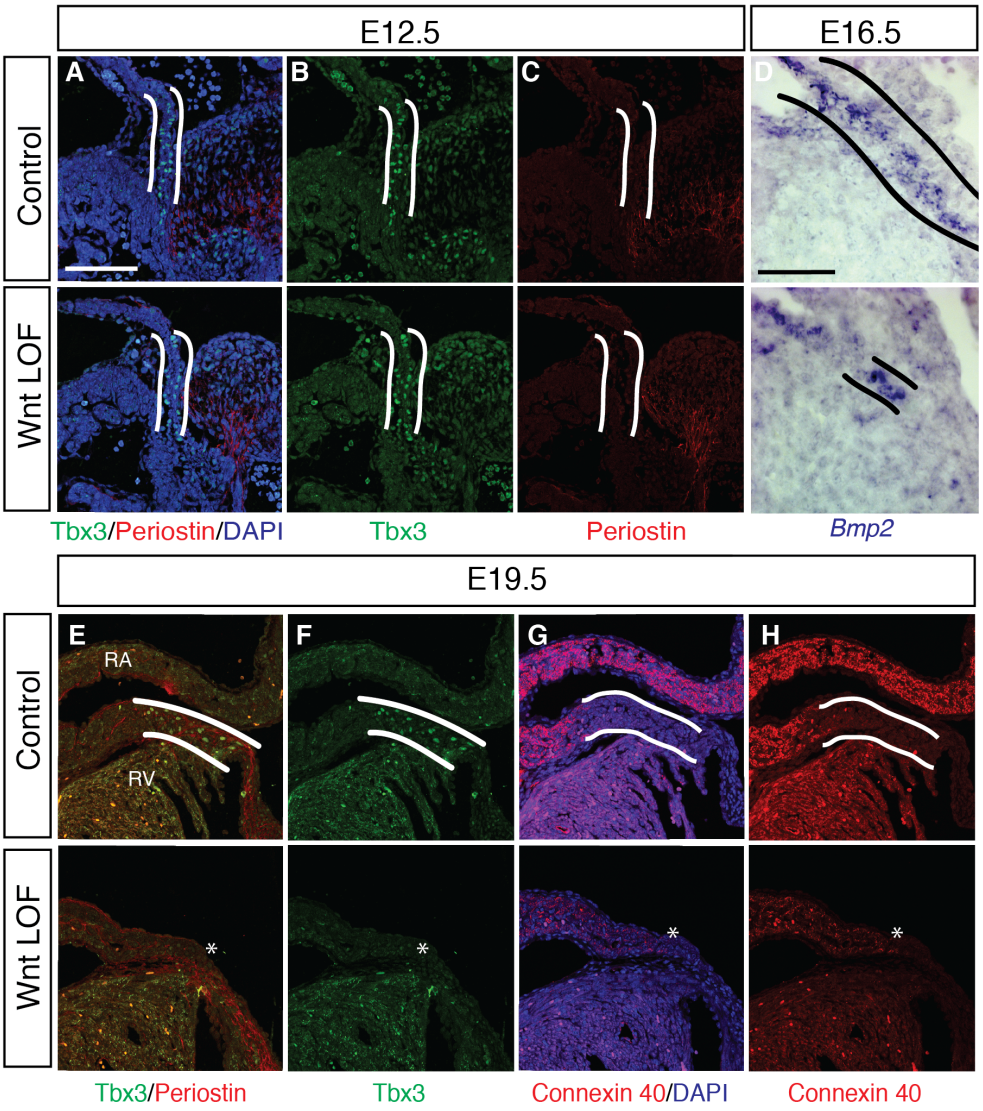

Figure 7. Progressive loss of AV canal myocardium in Wnt LOF embryos.
(A-C) Immunohistochemistry (IHC) for Tbx3 (AV canal myocardium) and periostin (a marker of fibroblasts undergoing epithelial to mesenchymal transition) demonstrate a grossly normal AVC structural organization at E12.5 in Wnt LOF when compared with control (A-C). (D) In situ hybridization demonstrates decreased *Bmp2* expression in Wnt LOF when compared with control (D) at E16.5. (E-H) By E19.5, IHC reveals a near absence of Tbx3+/Connexin 40- AVC myocardium in Wnt LOF mice when compared with controls (E-H). White outlines denote the AVC myocardium in control hearts, white asterisks denote the region between the right atrium and right ventricle where AVC myocardium is absent in Wnt LOF emrbyos. The sections shown in F are serial to E and the sections in H are serial to G. Scale bar for A also corresponds to panels B,C, E-H and is 100 μm. Scale bar in panel D is 50 μm.

The mechanism underlying Wnt's activity here remains unclear. Is Wnt signaling required for the continual specification of this tissue? Upon loss of Wnt signaling, does the AVC

myocardium transdifferentiate into other tissue? Alternatively, upon loss of canonical Wnt signaling, does the AVC myocardium undergo cell death?

2.4 Wnt is Not Required for Early Development of the AVC

Since the *αMHC-Cre* begins to be expressed only around E10.5, when the AVC has already developed, it cannot be used to determine if Wnt signaling is required for early development of this tissue. To address this question, I used the $Tbx2^{Cre}$ which is expressed in the AVC by E9.0, right before it fully develops. Despite the earlier activation of this Cre, at E10.5 the AVC was morphologically normal as was Tbx3 expression in that tissue (figure 8). It remains to be seen if Wnt signaling is required for initial specification of this tissue. Interestingly, Bressan et al have shown that Wnt signaling is required for SAN specification in the chick embryo[57]. It will be interesting to see if this paradigm holds true in the mouse and for the AVC tissue.

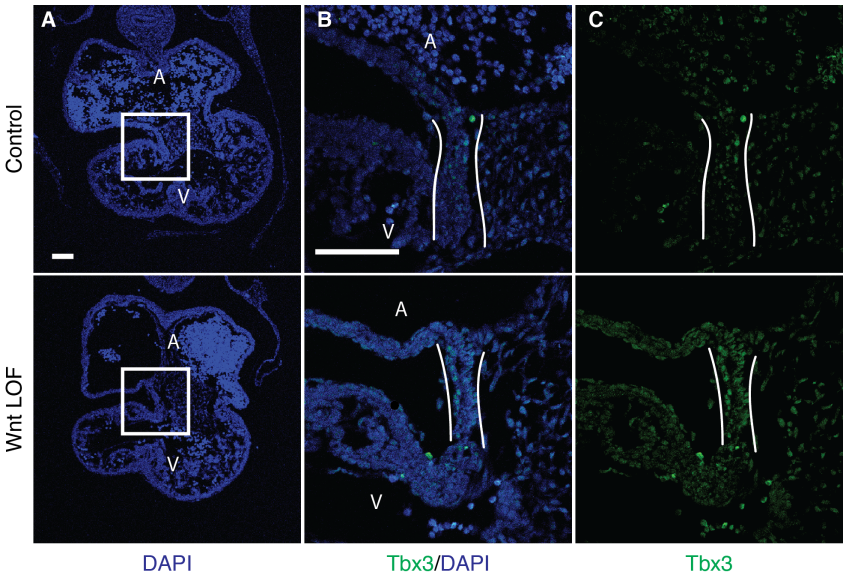

Figure 8. Canonical Wnt signaling is not required for early AVC maintenance.
Gross morphology is normal in $Tbx2^{Cre/+}$;$Ctnnb1^{dm/fl}$ embryos at E10.5 when compared with littermate controls (A) and Tbx3 expression is preserved (B,C). Scale bar in B corresponds to B,C and scale bars in A,B are 100 μm. Sections in B,C are magnified regions corresponding to the white box in A.

There are several important questions that remain unanswered. How does myocardial Wnt regulate the non-myocardial valve? Is there a secreted ligand, downstream of canonical Wnt

signaling that is required for valve maturation? An AVC explant assay[50] could be used to screen for those factors. Another area of interest lies in the role of Wnt in the tricuspid but not mitral valve. Why is Wnt required only for triscuspid valve development? This will be discussed in greater detail later in this dissertation along with other predominantly right sided phenotypes.

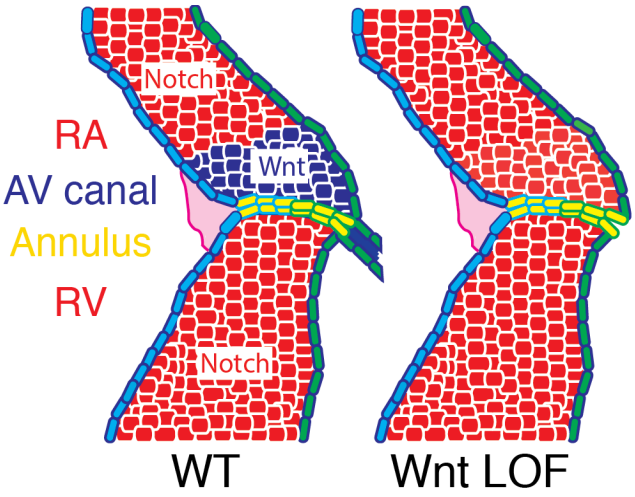

Figure 9. Model for the requirement of Wnt signaling in the AVC
Notch signaling is active in the atria and ventricles (red) whereas canonical Wnt signaling (blue) is normally expressed in the AVJ during development (WT) and is required for maintenance of the AV myocardial phenotype and proper formation of the tricuspid valve (Wnt LOF).

2.5 Contributions

Mouse breeding was done by Stephanie Hicks. *LacZ* staining, histological preparation, immunostaining, and in situ hybridization was done by Ben Gillers. Echocardiography was done by Attila Kovacs. Chapters 2-4, 6 published in altered form in Circulation Research 116(3):398.

Chapter 3: Wnt programs an AVJ phenotype

3.1 Wnt GOF Induces Ectopic AVJ Morphology

I have previously shown that myocardial loss of canonical Wnt signaling leads to loss of the AVC myocardium and is therefore required for its development. Based on this data, I asked if Wnt is sufficient to induce AVC development. To ask this question, I over activated canonical Wnt signaling using a floxed allele of *β-catenin* in which exon 3 is deleted in the presence of Cre [34]. I first used the $Mlc2v^{Cre}$. $Mlc2v^{Cre}$ is expressed in a subset of ventricular myocytes during development and in all ventricular myocytes in the adult.

One of the hallmarks of the AVC is the presence of the annulus fibrosis; an insulating plane of fibroblasts and adipocytes that insulates the atrial and ventricular myocardium [54]. This allows all electrical activity to funnel through the AVN. When Wnt was activated only in myocytes ectopic fibrofatty depositions developed in stochastic locations throughout the ventricles. These grooves are histologically indistinct from the normal AV groove. This suggests that activation of canonical Wnt signaling is sufficient to induce AVJ-like tissue. Using trichrome staining, one can see the fibrofatty deposition very clearly (figure 10A-C). To further validate that we are, in fact, seeing lipid containing cells, we used Oil-Red-O to stain these hearts. In control hearts, one can see a streak of adipocytes only in the posterior of the heart between the atria and ventricles. However, in the Wnt GOF, one can see patches of Oil-Red-O + tissue scattered throughout the ventricles (figure 10D,E). The phenotype seen here is reminiscent of the human disease, arrhythmogenic cardiomyopathy (AC); a condition characterized by ectopic fibrofatty deposition in the myocardium. Proteins of the ID in AC patients become deregulated and electrical

communication between myocytes is disturbed. This can lead to arrhythmias and sudden cardiac death.

3.2 Ectopic Fibrofatty Depositions are Not Myocyte Derived

There are several mouse models of this disease involving mutations in proteins of the ID. There are several suggestions in the literature that both in the human and mouse version of this disease, the adipocytes are derived from transdifferentiation of myocytes. Understanding the etiology of this disease is important for developing targeted therapies. Do we target the myocyte and prevent its transdifferentiation into a non-myocyte or do we target another cellular source such as epicardial cells. To address this question, I performed lineage tracing analysis to determine if, in fact, these ectopic adipocytes are myocyte derived. I used an $Mlc2v^{Cre/+};Ctnnb1^{fl(ex3)/+};R26^{TdTomato/+}$ mouse. In this mouse, only cells that once expressed *Mlc2v* would express both the over activated form of *β-catenin* and would fluoresce red due to *TdTomato* expression. Therefore, if a cell is red, it must have, by definition, either expressed *Mlc2v* at some point in its history or is the progeny of a cell that once expressed *Mlc2v*. In other words, if a cell is red, it either is, or once was, a myocyte. Therefore, if any adipocytes are TdTomato +, although they are no longer myocytes, they are myocyte derived. Oil-Red-O was used to detect adipocytes. Although, Oil-Red-O is a histological stain, I took advantage of the fact that it fluoresces upon far red excitation [58, 59] and therefore was able to look for colocalization of TdTomato and Oil-Red-O fluorescence .

Although many Oil-Red-O + cells were found, they did not express TdTomato (figure 10F-I). This suggests that in this mouse model of AC, the adipocytes are not myocyte derived. It remains to be seen what the cellular source of these adipocytes are. One interesting speculation is that they are epicardial derived. In fact, in the normal heart, several populations of AVJ cells are epicardial-derived [53, 54, 60, 61]. Both in vivo and in vitro lineage tracing experiments can be used to test this hypothesis here.

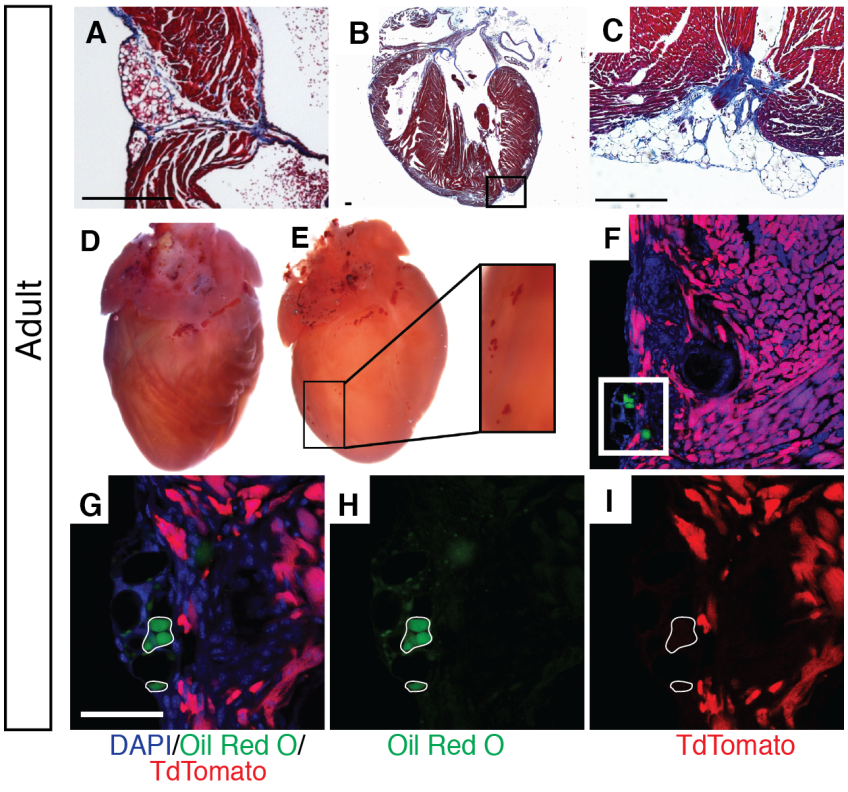

Figure 10. Ectopic Wnt activation induces an AVJ-like phenotype within the ventricles.
(A) Trichrome staining of the AV junction in a control adult heart, demonstrating a well delineated myocardial constriction, annulus fibrosis (blue), and subepicardial adipocytes. (B) *Mlc2v*$^{Cre/+}$; *Ctnnb1*$^{fl(ex3)/+}$ hearts (Wnt GOF) have ectopic myocardial constrictions containing an organized layer of fibroblasts and subepicardial adipocytes (boxed region from LV apex in B shown at higher magnification in panel C), which resemble the normal AV groove. (D,E) Oil-Red-O staining shows subepicardial adipocytes are very specific for the region of the AV junction in control mice (D), while Wnt GOF mice have regions of ectopic adipocytes within the ventricles (E). (F-I) Lineage tracing in Wnt GOF mice (*Mlc2v*$^{Cre/+}$;*R26R*$^{TdTom/+}$; *Ctnnb1*$^{fl(ex3)/+}$) demonstrates that ectopic fibro-fatty depositions (green) are not derived from Cre-expressing myocytes (red). Enlarged view of boxed region in F is shown in G-I to demonstrate that Oil-Red-O+ cells (green) are not colocalized with TdTomato+ cells (red). Scale bars 500 μm in A and C, scale bar for G corresponds to G-I and is 50 μm,

3.3 Wnt GOF Induces an AVJ Electrical Phenotype

Since Wnt GOF induces an AVJ morphology, we wanted to test the hypothesis that it also changes its function. The hallmark of the AVJ is slow conducting myocardium. The purpose of this is to delay the impulse as it travels from the atria to the ventricles allowing non-simultaneous contraction of these regions of the heart. In the embryo, this delay occurs through slow conducting canal tissue. In the adult, this occurs through insulation of the atria and ventricles via the annulus fibrosis and slow conducting myocardium in the AVN [62]. To test this, we used optical mapping to measure the conduction velocity in langendorf perfused hearts both in sinus rhythm and in programmed stimulation. In Wnt GOF, in both protocols, the conduction velocity is markedly decreased (figure 12C-K). In addition, the QRS is widened (figure 12A,B and 13B). Interestingly, the PR interval was also elongated (figure 13A). This suggests that Wnt GOF induces AVJ properties on the ventricular myocardium. Interestingly, it also induced heterogeneous conduction, which can be seen as a non-linear traverse of the impulse throughout the myocardium. Unexpectedly, when the RV was paced at cycle lengths shorter than 125 ms, the tissue was unexcitable (figure 12K). The refractory period is the time at which the cells in a given tissue are unexcitable, while they regenerate their ability to become excited. One of the properties of nodal tissue is its longer refractory period relative to working myocardium. This inexcitability suggests a longer refractory period and further strengthens my argument that Wnt GOF programs an AVJ/nodal phenotype on working myocardium.

Interesting differences between the right and left ventricle present in 2 forms here: 1) conduction velocity is slower in the RV than the LV 2) The RV was more unexcitable than the LV. Are these two differences related? Could differences in expression of gap junctions and sodium

channels at baseline explain a differential sensitivity to Wnt GOF? This will require further experiments to dissect.

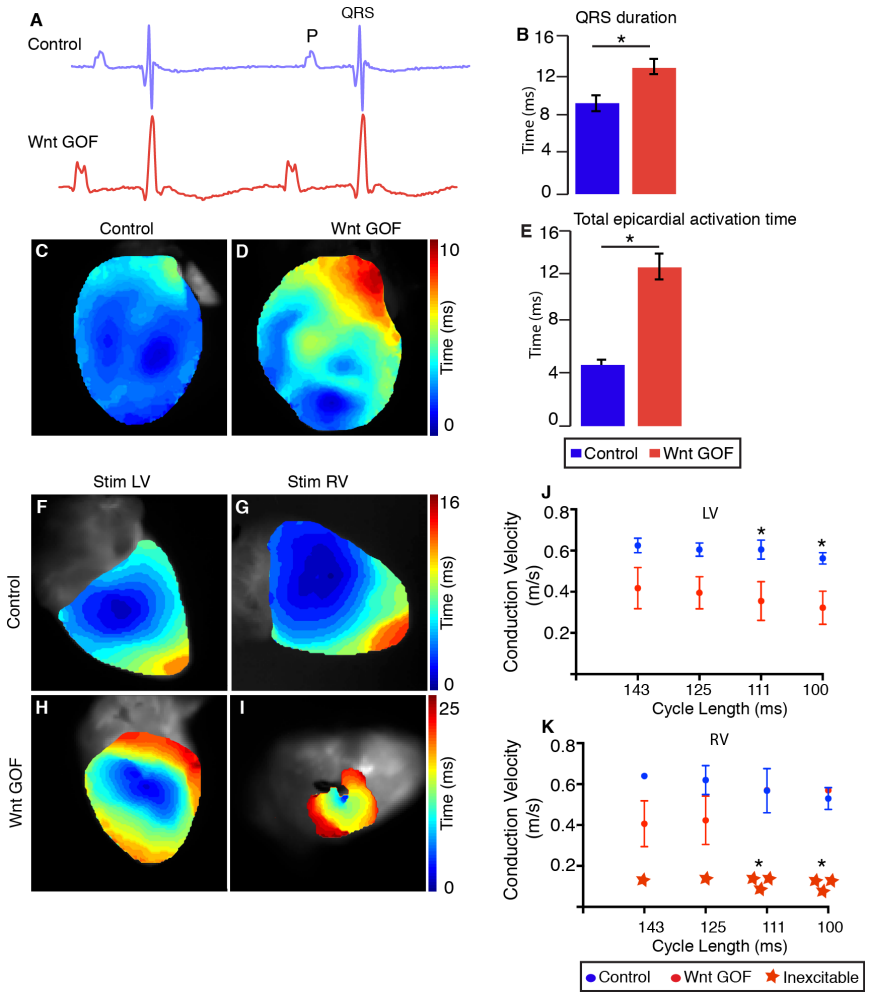

Figure 11. Ectopic Wnt activation programs ventricular myocytes to adopt an AVJ electrical phenotype. (A) Representative surface EKG from control (top) and *Mlc2v*$^{Cre/+}$; *Ctnnb1*$^{fl(ex3)/+}$ Wnt GOF (bottom) mice. (B) Wnt GOF mice have a prolonged QRS complex when compared with control littermates (9.2 ± 0.4 versus 12.6 ± 1.2 ms, n=5 each genotype). (C,D) Reconstructed electrical activation pattern from optical mapping experiment during sinus rhythm in control (C) and Wnt GOF (D) mice. (E) Total epicardial activation time is significantly prolonged in Wnt GOF mice (4.4 ± 0.4 versus 11.5 ± 1.0 ms, n=4 each genotype). (F-I) Representative electrical activation pattern of the LV and RV during epicardial stimulation in control (F,G) and Wnt GOF (H,I) mice. (J) Left ventricular (LV) longitudinal conduction velocity of Wnt GOF mice was slower during stimulation at each cycle length, and the difference between the two genotypes became larger at faster pacing rates (111 and 100 ms cycle lengths, n=4). (K) Right ventricular (RV) longitudinal conduction velocity of Wnt GOF mice was also slower, and was more severely decreased than in the LV. One Wnt GOF mutant had an electrically inexcitable RV when paced at 143 ms cycle length, while two others had markedly decreased conduction velocity at slower cycle lengths and became inexcitable at pacing rates above 125 ms cycle interval. This is consistent with decremental conduction, a property of AV canal and AV nodal tissues. Note the different time scales between each experiment. Data are represented as mean ± SEM. Group comparison for conduction velocity was performed using a Student's unpaired 2-tailed t-test at each cycle length. Group comparison for inexcitability was performed using a Chi squared test without yates correction. *p<0.05.

The PR interval elongation is particularly intriguing since, as mentioned in the introduction, Notch activation decreases the PR interval. This leads to the possibility that Notch and Wnt have

apposing affects on tissue specification and properties. This will be further discussed in chapter 4.

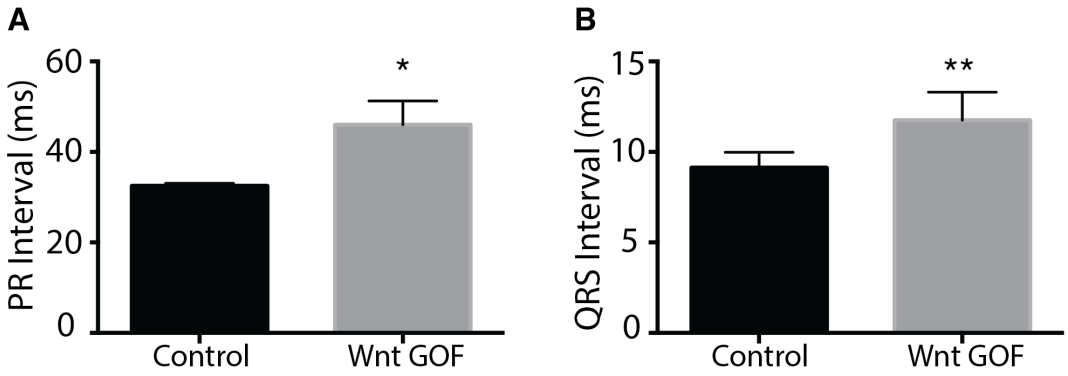

Figure 12. PR interval and QRS interval prolongation in Wnt GOF mice.
(A) The PR interval is prolonged in Wnt GOF mice (46.0 ± 2.6 ms) when compared with littermate controls (32.5 ± 0.3 ms) as measured by surface ECG. (B) The QRS interval is prolonged in Wnt GOF mice (11.7 ± 0.8 ms) when compared with littermate controls (9.1 ± 0.4ms) as measured by surface ECG. n=4, *$p<0.005$, **$p<0.05$. Data are expressed as mean ± SEM. Group comparison was performed using a Student's unpaired 2-tailed t-test.

3.4 Wnt GOF Downregulates Working Myocardium Gene Expression

I hypothesized that the decrease in conduction velocity may either be due to the fibrofatty deposition or altered gene expression. The fibrofatty deposition may serve to impede the electrical impulse as it travels through the tissue. This may also explain the heterogeneous conduction. The presence of non-conducting tissue may force the impulse to change its path and therefore traverse the tissue in a non-linear fashion.

To determine if altered gene expression may also be involved, we assayed connexin and sodium channel gene expression. Connexins are primarily localized to the IDs and form gap junctions-allowing electrical communication between cells [55]. Abnormal connexin deposition could lead to both slower and heterogeneous conduction. Additionally, lower connexin levels could have a similar effect. Since Cx43 is the main high conductance gap junction protein in the ventricle, we

focused on this protein [63]. While immunostaining did not reveal abnormal Cx43 localization, qPCR did reveal lower *Cx43* mRNA levels in the Wnt GOF ventricles (figure 11A).

Since sodium channels play an important role in regulating conduction velocity, we next assayed mRNA levels for *Scn5a*, one of the main sodium channels in the heart [59, 64]. In fact, mutations in *Scn5a* have been associated with numerous human cardiac diseases including Brugada Syndrome [59]. qPCR reveled that Wnt GOF downregulated *Scn5a* mRNA levels by 50% (figure 11A).

It remains to be seen which of these factors are essential in Wnt mediated slowed conduction velocity. One could envision a rescue experiment in which either *Cx43* or *Scn5a* is unregulated in a Wnt GOF mouse. If upregulation of either one is sufficient to rescue the delayed conduction velocity, one would conclude which is important for this phenotype. It further remains to be seen if this altered gene expression is sufficient to alter conduction velocity or if the fibrofatty deposition is required for this phenotype. While it has been shown that downregulation of either *Cx43* or *Scn5a* is sufficient to decrease conduction velocity [64], are the decreased message levels in the Wnt GOF sufficient for this phenotype? Answering these questions will be important for developing targeted therapies to treat AC.

It is also important to note that while this altered gene expression can explain the conduction velocity phenotype, it is also important in understanding how far Wnt GOF programs an AVJ phenotype. As I have previously shown, Wnt GOF induces AVJ morphology and function. The altered gene expression is further consistent with this characterization.

The decreased *Cx43* and *Scn5a* levels are crucial for understanding this mouse model of AC. Adult mice that have fibrofatty deposition and decreased conduction velocity, also have this altered gap junction and sodium channel profile. It is important to understand, though, if this results from a developmental gene program gone awry or an unrelated process. This approach to understanding disease is an important paradigm not limited to the cardiovascular space. In fact, much of cancer can be understood in terms of developmental processes gone awry such as abnormal EMT leading to tumor metastasis. Therefore, the same processes that are required for AVJ development, such as Tbx3 dependent patterning, may be deregulated and causal of the AC phenotype.

To dissect this, we used a different Cre driver to overactivate Wnt signaling. The $Mlc2v^{Cre}$ is expressed in a subset of ventricular myocytes during development and only in the adult is it expressed in all ventricular myocytes. Use of this Cre allows survival to adulthood in a phenotype that is otherwise embryonic lethal. We therefore used this Cre in the above described experiments. However, since it is not expressed in all myocytes during development [19], one may miss certain important biological information using this Cre. We therefore used the *αMHC-Cre* to activate Wnt signaling for this next experiment. *αMHC-Cre* is expressed in almost all myocytes during development and therefore is more useful in assessing changes in gene expression [20].

To analyze the etiology of this phenotype, we assayed for ectopic Tbx3 expression. As described earlier, Tbx3 is a prominent member of the Tbox family of transcription factors. Tbx3 is required for normal development of the AVC and its expression marks both canal and nodal tissue [6, 10, 65,

[66]. Importantly, it is expressed very early in development and can be seen as one of the master regulators of AVC development. I also analyzed periostin localization. There is a very unique and distinct localization pattern of periostin and Tbx3 in the developing AVC and node. While Tbx3 is expressed in nodal and canal myocytes, periostin is secreted specifically by non-myocytes in the node and canal. Periostin expressing cells deposit a spider web like network of periostin surrounding and intertwining with Tbx3 positive cells. If the downregulation of *Cx43* and *Scn5a* are not regulated here by Tbx3 in the same way the AVJ is specified, one would expect to see no ectopic Tbx3.

In Wnt GOF, not only did we see upregulation of *Tbx3* mRNA in the embryo (figure 11B), I also detected ectopic Tbx3 and periostin protein in the apex of the embryonic LV in an expression pattern reminiscent to that of the canal/node (figure 11C-H). This leads to the very intriguing hypothesis that the AC phenotype seen in Wnt GOF mice is in fact, a developmental process gone awry that now occurs, due to ectopic Wnt activation, in sporadic locations throughout the ventricle instead of being limited to the AVC/N. One can speculate that the human AC disease develops in a similar manner. This again, is an important question not only for understanding the role of Wnt but for developing targeted therapies. Instinct may suggest that treatment of AC should occur through targeting gap junctions or other ID proteins. Based on these data, one can imagine that targeting the developmental processes or genes such as *Tbx3* or Wnt signaling, may in fact, present a more powerful form of a therapy.

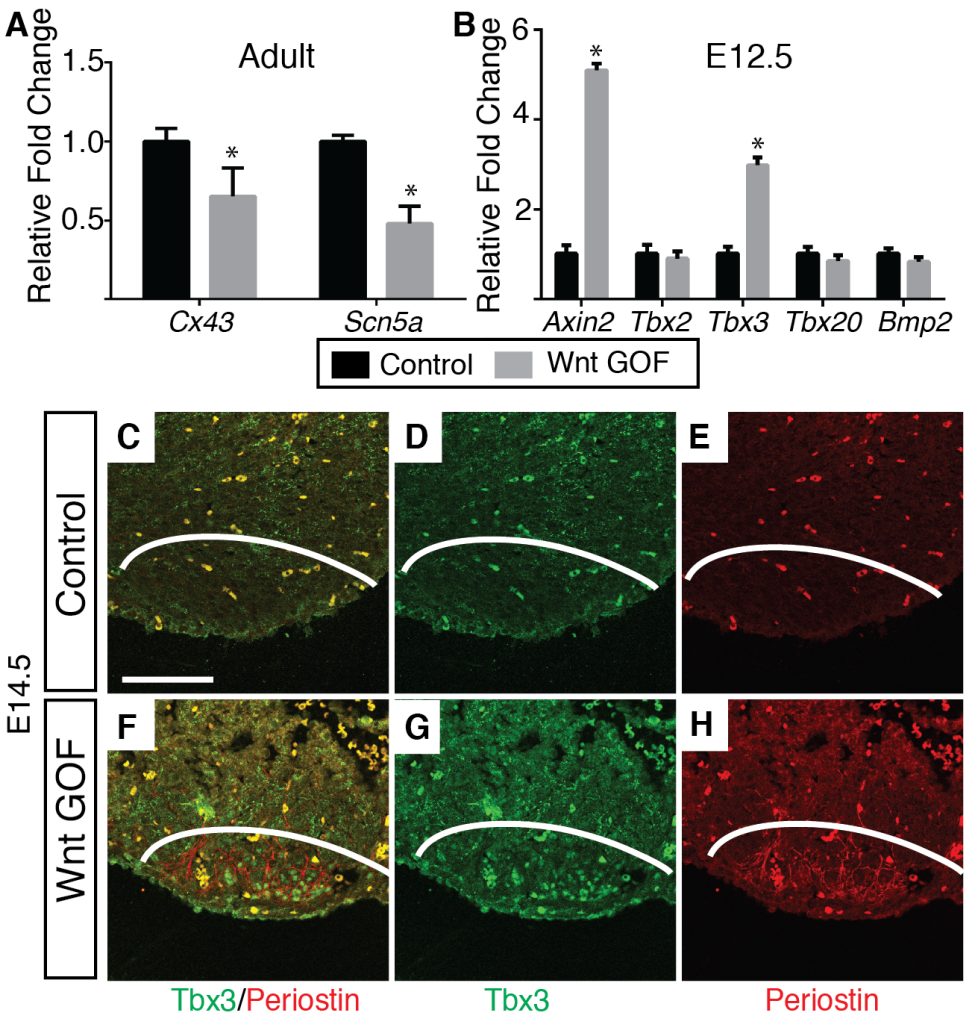

Figure 13. Ectopic Wnt activation induces an AVJ-like phenotype within the ventricles.
(A) Expression of *Cx43* and *Scn5a*, which regulate conduction velocity, are significantly decreased in the LV of adult Wnt GOF mice when compared with littermate controls (n=3 each genotype). (B) Expression of *Axin2* and Tbx3 are upregulated in ventricles from E12.5 Wnt GOF mice (*αMHC-Cre;Ctnnb1*$^{fl(ex3)/+}$) when compared with littermate controls (n=7 each genotype), while *Tbx2*, *Tbx20* and *Bmp2* are unchanged. (C-H) IHC of E14.5 embryos demonstrates ectopic Tbx3 and periostin near the ventricular apex in Wnt GOF mice when compared with littermate controls (white line demarcates the apex in both genotypes, n=3). Scale bar in C corresponds to C-H and is 100 μm. Data are represented as mean ± SEM. Group comparison was performed using a Student's unpaired 2-tailed t-test. *p<0.05.

3.5 Adult Activation of Wnt Signaling Downregulates *Scn5a*

It is well known that as an organism develops, it loses a great deal of plasticity. This may have an evolutionary benefit; once the organism has developed this can prevent gross susceptibility to disease [67]. Therefore, once the developmental pathways have been used to program the organism, they become epigenetically silenced for its protection. I therefore wanted to determine the adult

susceptibility to this AVJ phenotype in response to increased Wnt signaling. Previously, both using *Mlc2v* and *αMHC-Cre* mice, Wnt is activated embryonically. I therefore used a doxycycline inducible system to interrogate the affects of Wnt when activated only in the adult.

To do this, I used an *αMHC-rtTA;tetO-Cre;Ctnnb1*$^{fl(ex3)/+}$. Only in the presence of doxycycline can the myocyte specific rtTA enter the nucleus and activate Cre expression that in turn, deletes exon3 of *β-catenin*. The downside of this system is that, even though it is doxycycline inducible, since Cre mediated genetic recombination occurs, Wnt overactivation cannot be turned off.

After adult mice were fed doxycycline chow for three weeks, each chamber of the heart was harvested and analyzed via qPCR. Importantly, *Scn5a* was downregulated 5-fold in the LA and *Cx40* was downregulated 2-fold in the RA (figure 14A,B). While *Cx43* is the main gap junction in the ventricles, *Cx40* is predominant in the atria. This suggests that Wnt regulation of gap junctions is not specific to *Cx43* in the ventricle as described before, but may represent a more global role of Wnt's regulation of this class of proteins. This suggests that Wnt signaling, even when activated in the adult, has the capacity to regulate the cardiac electrical gene program. It remains to be seen if inducible Wnt GOF also causes a slowing of conduction velocity.

Interestingly, while there was a trend for upregulation of *Tbx3* in the RA, those changes are not statistically significant. This suggests that adult activation of Wnt signaling may not occur through the developmental paradigm described before. Alternatively, there may be an initial increase in *Tbx3* expression which is resolved before the three week timepoint when the hearts were harvested.

Of further note, while *Scn5a* was dramatically decreased in the LA, it was not in the RA. One can speculate why there are such differences between the RA and LA. Gene expression differences between chambers has long been noted [68] . One possibility here, is that contamination of the SAN, contained within the RA sample may give one a mistaken understanding of the expression changes. This is because the SAN has a very different expression profile than both the LA and the RA [69] highlighted in figure 14C. Alternatively, the presence of the SAN, which may already have high levels of Wnt signaling, may cause that chamber to respond differently to activation of Wnt than the LA, which is segregated from Wnt activity in the adult.

Interestingly, *Tbx18* expression is not affected in the RA nor LA. Several studies have shown the sufficiency of *Tbx18* to reprogram a nodal phenotype in isolated myocytes and in vivo in both guinea pig and porcine models. Based on the data I have shown here, it is clear that Wnt signaling is sufficient to reprogram at, least in part, a nodal phenotype. An important question that remains is how do *Tbx18* and Wnt signaling relate to each other. Is one upstream of the other or do they function in parallel pathways. My data here suggests that, at least in the atria, Wnt signaling is not upstream of *Tbx18*. It remains to be seen if it is downstream or functions in a separate pathway.

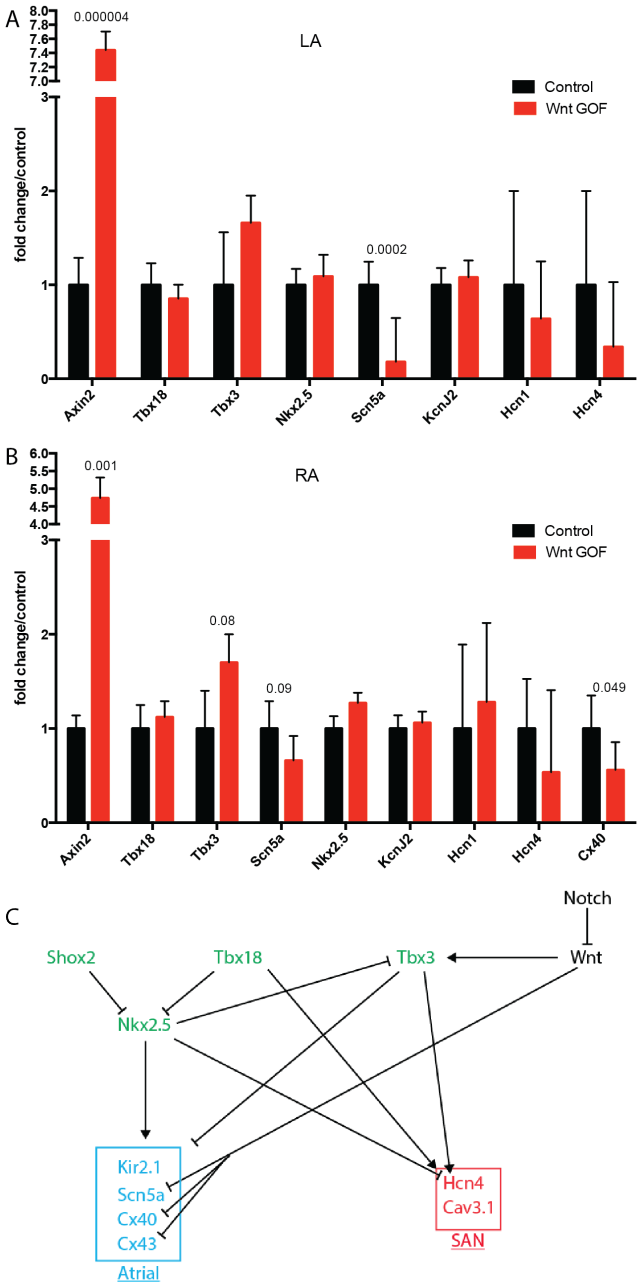

Figure 14. Adult activation of canonical Wnt signaling downregulates working myocardium gene expression.
Wnt signaling was activated in the adult using the *αMHC-rtTA; tetO-Cre; Ctnnb1*$^{fl(ex3)/+}$. Mice were fed doxycycline starting at 3 weeks and sacrificed at 6 weeks and analyzed with qPCR. (A) In the LA, *Scn5a* is downregulated 5 fold. (B) In the RA, while *Scn5a* is not downregulated, *Cx40* is decreased by 50%. *Tbx3* trends towards an increase but is not statistically significant**.** *Axin2,* a direct transcriptional target of canonical Wnt signaling, is highly unregulated in both LA and RA. N=6. Data are represented as mean ± SEM. Group comparison was performed using a Student's unpaired 2-tailed t-test. P values, where significant or close to significance, are written above the bar. (C) Map of the ion channels expressed in working myocardium (atrial, blue) and SAN myocardium (SAN, red) and the genetic network that establishes theses two different expression patterns.

It is clear now that activation of canonical Wnt signaling is sufficient to program an AVJ phenotype. This is evidenced by an AVJ gene profile, morphology, and electrical phenotype. The role of developmental pathways in this phenotype is highlighted by ectopic Tbx3 expression. This understanding may highlight important therapeutic directions to explore in the treatment of

AC. Interestingly, several studies have suggested that Wnt LOF is causal of the AC phenotype and have even raised the possibility of treating AC via upregulation of Wnt signaling [30, 70]. My data here is very clear, that at least in mice, Wnt GOF can actually be causal of the AC phenotype. It is possible that imbalance of Wnt signaling, in either direction, can cause this disease. Alternatively, Wnt signaling, at different points in development may have opposite effects. Either way, we need to be very cautious in treating AC with Wnt agonists before getting a better understanding of the mechanism(s) of Wnt induced AC.

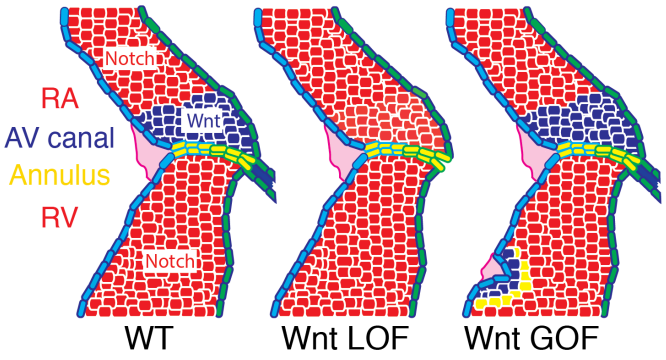

Figure 15. Model for Programming the AVJ via Wnt LOF and GOF
Notch signaling is active in the atria and ventricles (red) whereas canonical Wnt signaling (blue) is normally expressed in the AV junction during development (WT) and is required for maintenance of the AV myocardial phenotype and proper formation of the tricuspid valve (Wnt LOF). Ectopic Wnt activation within ventricular myocardium (Wnt GOF) is sufficient to induce *Tbx3* expression and ectopic AV junction properties as assessed by morphologic and electrical criteria.

3.6 Contributions

Histological preparation and trichrome staining were done by Stephanie Hicks and Ben Gillers. Oil-Red-O staining was done by Haytham Aly and Ben Gillers. Immunostaining was done by Ben Gillers. qPCR was done by Aditi Chiplunkar and Ben Gillers. EKGs were done by Baas Boukens, Stephanie Hicks, and Ben Gillers. Optical mapping and associated analysis was done by Baas Boukens.

Chapter 4: Wnt Signaling is Inhibited by Notch Signaling

4.1 Notch Signaling Downregulates Canonical Wnt Signaling

I have shown that canonical Wnt signaling is both necessary and sufficient for development of the AVJ. Furthermore, I have shown that Canonical Wnt signaling is upstream of Tbx3 signaling in development of this tissue. What regulates canonical Wnt signaling and why is it so specific to this region? Although there is some active Wnt signaling elsewhere the heart, the strongest region of Wnt signaling is in the AVC.

It has been reported that during development, Notch signaling is active in the working myocardium. The direct Notch targets, *Hey1* and *Hey2* are highly expressed in the developing atria and ventricles, respectively [41, 71]. Importantly, Notch is not active in the AVC. Because Notch and Wnt are active in the heart in primarily a mutually exclusive pattern, I hypothesized that either Notch inhibits Wnt activity or vice versa. Furthermore, activation of Notch and Wnt signaling have opposite effects on the PR interval. While Notch activation decreases the PR interval, activation of Wnt signaling elongates it. Therefore, there is strong basis to speculate that one of these pathways inhibits the other. To test the hypothesis that Notch signaling inhibits canonical Wnt signaling, I utilized the doxycycline inducible system to overexpress the Notch Intracellular Domain (NICD) in myocytes. When mated with the *Axin2*^{LacZ} mice, I was able to assay altered Wnt activity upon Notch activation.

In control mice, Wnt is active in both the AVC myocardium and valve tissue. However, upon activation of Notch signaling, while valve *Axin2* is unaffected, its expression in the AVC myocardium is greatly reduced. I used qPCR to quantify this reduction and found that while *Hey1* and *Hey2* are dramatically increased in Notch GOF, *Axin2* is reduced by 50% (figure 16A,B). Presumably, the presence of valve tissue in the preparation diminished the perceived reduction of *Axin2* expression. Also of note, the Wnt target, *Gata6* is also reduced (figure 16A).

These data suggest that Notch GOF inhibits Wnt activity. Importantly, *β-catenin* transcript levels are not changed, suggesting that this occurs through a post transcriptional mechanism (figure 16A). The inhibitory effect of Notch on Wnt signaling is an emerging paradigm in several environments. For example, Kwon et al have shown that Notch signaling inhibits canonical Wnt singling in myocyte progenitor cells using Isl1 to mark this population [23, 72]. Kwon suggests the mechanisms occurs through Notch targeting β-catenin for lysosomal degradation. It remains to be seen if this or other mechanisms are responsible for the AVC phenotype.

Given that Notch signaling is able to suppress Wnt activity, one may hypothesize that the relative absence of Wnt activity outside of the AVC during normal embryonic development may be due to the presence of endogenous Notch signaling. To further elucidate this, it would be worthwhile to investigate the levels of *Axin2* in the Notch LOF mouse such as a Hey2 knockout or the dominant negative MAML mouse, a Notch LOF model.

4.2 Notch Signaling Inhibits the AVJ Phenotype

I have previously shown that Canonical Wnt signaling is required for normal AVC development. Since Notch GOF downregulates canonical Wnt signaling, I hypothesized that upon Notch GOF,

the AVC myocardium would be perturbed. Interestingly, in Notch GOF mice, there is a reduction in Tbx3 expression as assed both by qPCR and immunofluorescence (figure 16A,C,D). This suggests that Notch activation downregulates both canonical Wnt signaling and destabilizes the AVC myocardium. Interestingly, Notch activation also downregulates *Tbx20*, another important regulator of AVC development (figure 16A). Since *Tbx20* is not affected in the Wnt LOF or GOF models, this would suggests that Notch activation has additional affects on this tissue besides regulation of Canonical Wnt signaling.

Interestingly, it has been reported that mice lacking *Tbx20* develop a complete common AVC [52]. The Notch GOF mice do not display this phenotype. This may be due to late activation of Notch signaling or only partial downregulation of *Tbx20*.

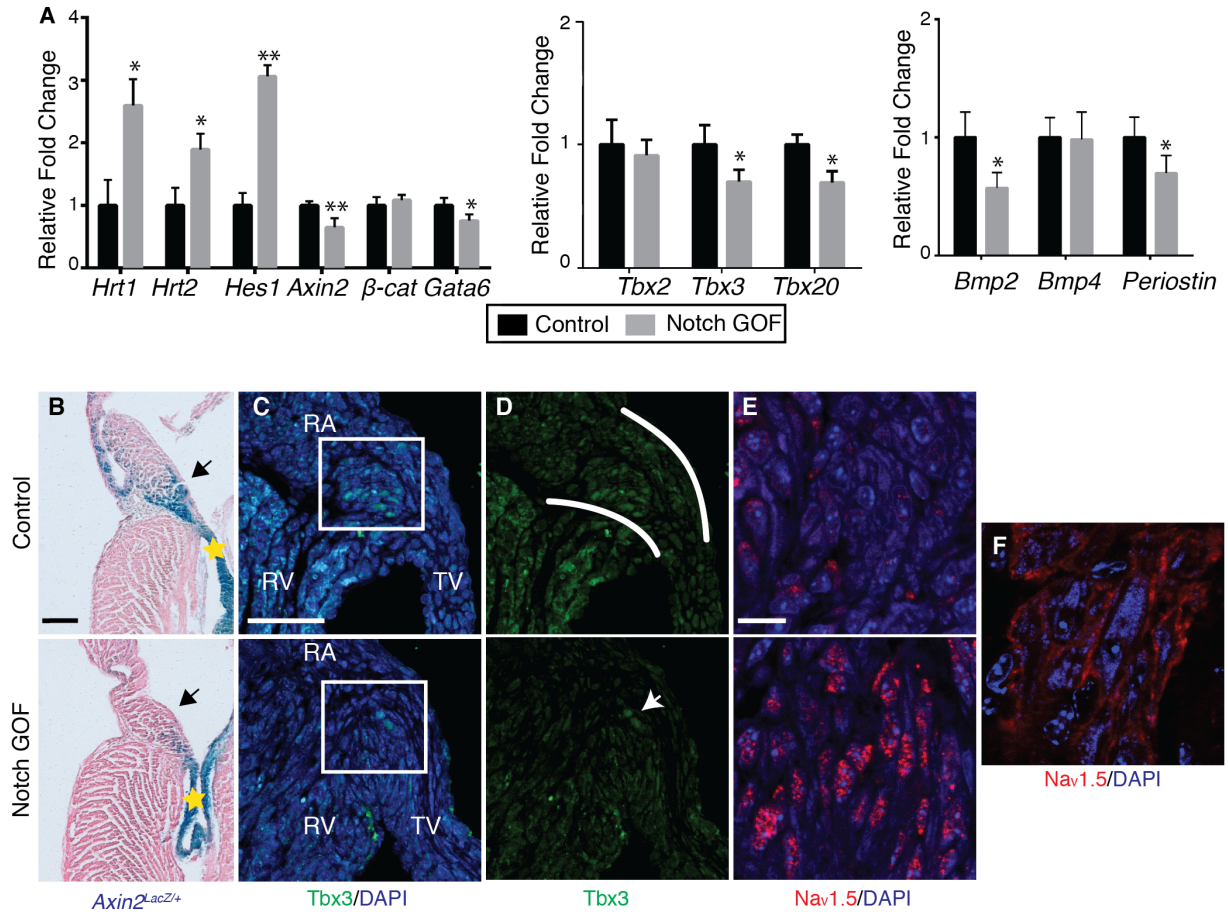

Figure 16. Perinatal Notch activation reprograms the AVJ into chamber-like myocardium.
(A) Transient activation of Notch signaling in the myocardium through administration of doxycycline (DOX) to *αMHC-Cre; tetO-NICD* double transgenic mice from E17.5 until P1 (Notch GOF) upregulates direct Notch targets and downregulates Wnt targets *Axin2* and *Gata6*, as measured by RT-qPCR. Important regulators of the AV junction, including *Tbx3*, *Tbx20*, *Bmp2*, and *periostin* are also downregulated (n=8 each genotype). (B) Histological sections of $Axin2^{LacZ/+}$ hearts show active canonical Wnt signaling in AV junctional myocardium and tricuspid valve mesenchyme at P3. Notch GOF downregulates $Axin2^{LacZ/+}$ expression in the AV junctional myocardium but does not affect expression in the valve mesenchyme. (C-E) IHC demonstrates decreased Tbx3+ AV junctional myocardium in Notch GOF mice when compared with littermate controls (C,D). IHC demonstrates ectopic Nav1.5 in Notch GOF AV junctional myocardium while Nav1.5 is absent within the AV junctional myocardium in littermate controls (E). (F) Membrane localization of Nav1.5 is shown in control atria for comparison. TV=tricuspid valve, RA=right atrium, RV=right ventricle. Data are expressed as mean ± SEM. Group comparison was performed using a Student's unpaired 2-tailed t-test. *p<0.05. **p<0.001. Scale bars in B,C are 100 μm. Scale bar in C corresponds to C,D . Scale bar in E corresponds to E,F and is 10 um. Black arrows in B denote AV junctional myocardium, and stars in B denote the tricuspid valve. White lines in D demarcate the AV junctional myocardium. Arrow in D denotes the sparse Tbx3+ region in Notch GOF. Sections in E are serial to C,D and represents a magnified region corresponding to the white box in C.

4.3 Wnt Signaling Rescues Notch Induced Accessory Pathway Formation and Ventricular Preexcitation

Our lab has previously shown that using the *Mlc2v*^{Cre}, Notch GOF mice develop accessory pathways and ventricular preexcitation [18]. Since Notch signaling downregulates Wnt signaling, I asked whether this downregulation of Wnt was required for Notch induced preexcitation. To test this, we used *Mlc2v*^{Cre} to activate both NICD and *Ctnnb1*$^{fl(ex3)}$, the Wnt GOF allele described earlier. While 100% of Notch GOF mice display this phenotype, 25% of the double mutant mice display a complete rescue. As can be seen from the ECG traces, the PR interval is normal in this rescue. Accessory pathway formation is also rescued in 25% of mice. As can be seen in the trichrome staining, an AV groove and annulus are clearly seen in WT mice. In Notch GOF mice, the groove and annulus are lost and an accessory pathway is seen. In the rescue mice, the groove and annulus are present and there is no hint of an accessory pathway (figure 17). These data suggest that downregulation of canonical Wnt signaling is required for development of Notch induced ventricular preexcitation.

To test whether loss of Wnt alone is sufficient for development of this pathology, we used the *Mlc2v*^{Cre} to delete *β-catenin*. When using 2 floxed alleles of *β-catenin*, mice are embryonic lethal and we could not test for ventricular preexcitation. However, when using one floxed allele and one DM allele, mice survived to adulthood. However, there was no PR interval shortening suggesting that while loss of canonical Wnt signaling is required for development of Notch induced preexcitation, it is not sufficient (figure 18). This again suggests that Notch activation regulates more in the AVJ than Wnt signaling alone. One candidate for this is *Tbx20*, which as I have already shown, is downregulated upon Notch activation. It remains to be seen if

simultaneous downregulation of canonical Wnt signaling and *Tbx20* is sufficient for development of preexcitation.

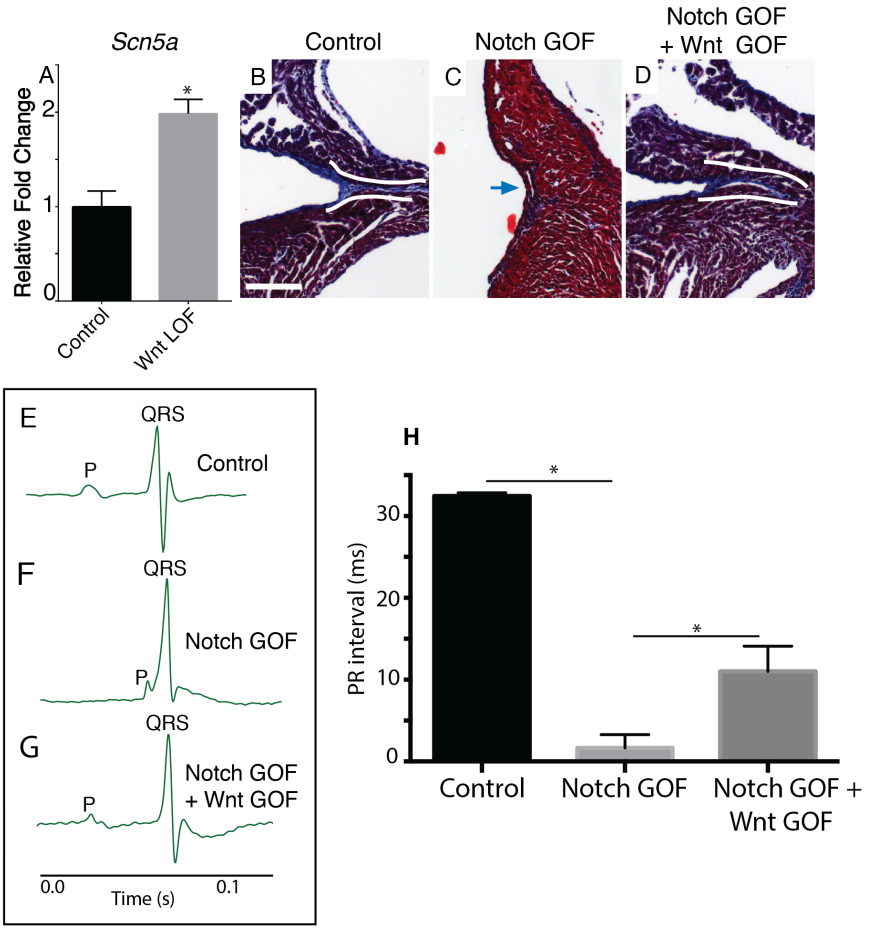

Figure 17. Inhibition of Canonical Wnt signaling is required for Notch induced ventricular preexcitation. (A) RT-qPCR from the LV of adult *Mlc2v*$^{Cre/+}$*; Ctnnb1*$^{dm/fl}$ Wnt LOF mice demonstrates upregulation of *Scn5a* when compared with littermate controls, demonstrating a requirement for Wnt signaling in normal ion channel gene regulation. (B-D) Trichrome-stained section from a control heart demonstrates a deep myocardial constriction between right atrium and right ventricle with a well-formed annulus fibrosis (B, annulus denoted between white lines). Notch GOF mice (*Mlc2v*$^{Cre/+}$*; NICD*) have accessory pathways, disorganized annular tissue, and lose their AV constriction (C, arrow denotes accessory pathway). Simultaneous activation of Wnt signaling on the background of Notch GOF (*Mlc2v*$^{Cre/+}$*; Ctnnb1*$^{fl(ex3)/+}$*; NICD*) rescues the morphology of the AV junction, including the formation of the annulus fibrosis and the AV constriction (D). (E-G) Representative EKG traces show that Notch GOF mice have severe PR interval shortening and a delta wave, characteristic of ventricular preexcitation (F) when compared with control (E). The PR interval is completely rescued and comparable to control littermates in 25% of Notch GOF + Wnt GOF mice (G). There is a partial rescue of the PR interval in the remaining mice (H). Scale bar in B corresponds to B,C,D and is 100 μm. Data are expressed as mean ± SEM. Group comparison in A was performed using a Student's unpaired 2-tailed t-test. Group comparison in H was performed using a one-way ANOVA followed by a post-hoc Tukey's test. $p<0.05$, $n>20$.*$p<0.05$.

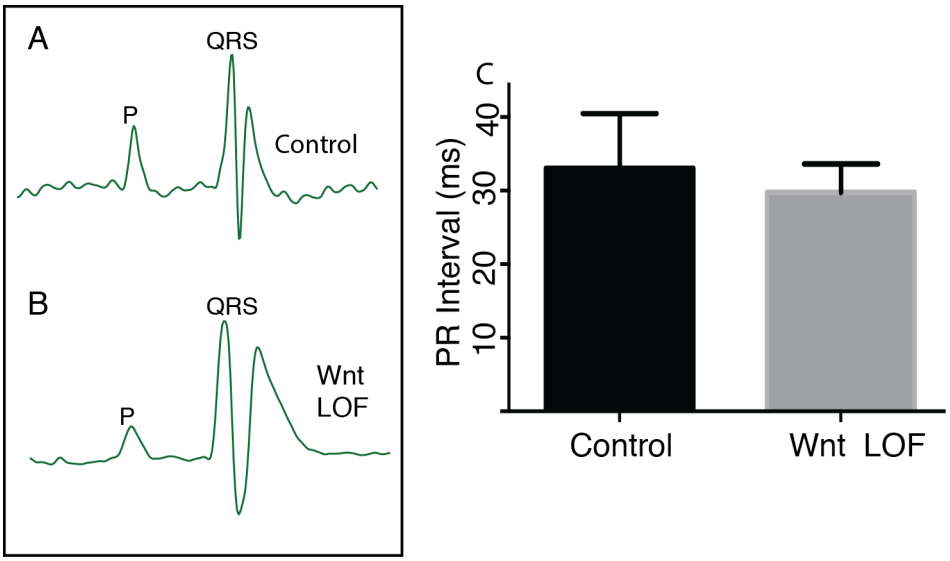

Figure 18. Wnt LOF is not sufficient for the development of ventricular preexcitation.
(A,B) Representative surface EKG from control (A) and *Mlc2v*$^{Cre/+}$; Ctnnb1$^{dm/fl}$ Wnt LOF adult mice (B), demonstrating a normal PR interval. (C) There is no difference in the PR interval between control and Wnt GOF mice (n=8 each genotype). Data are expressed as mean ± SEM. Group comparison was performed using a Student's unpaired 2-tailed t-test.

4.4 Wnt GOF Rescues Notch GOF Induced Gene Expression

Upon activation of Notch signaling, I previously showed that there is a decrease in canonical Wnt signaling and the AVC marker, *Tbx3*. I asked whether Notch also regulates sodium channel signaling. *Scn5a* is highly expressed in working myocardium and is absent from the AVJ. Interestingly, as can be seen with immunofluorescence, Notch activation induces ectopic $Na_v1.5$ (the translated protein of *Scn5a)* in the AVC region (figure 16E). Furthermore, by qPCR, we found that Notch activation upregulates *Scn5a* levels (figure 19). Since we already showed that Wnt GOF downregulates *Scn5a* levels, we asked whether simultaneous activation of Notch and Wnt would up- or downregulate *Scn5a*. We found that Wnt GOF is able to rescue the Notch induced upregulation of *Scn5a* (figure 19). This shows that canonical Wnt signaling is not only required for Notch induced ventricular preexcitation but also for its upregulation of *Scn5a*. This further highlights that the mode of action of these Notch induced phenotypes is likely via downregulation of canonical Wnt signaling.

Figure 19. Wnt activation rescues Notch induced regulation of *Scn5a*

Wnt and Notch cooperatively regulate *Scn5a* gene expression in adult LV as measured by qPCR. Notch GOF upregulates *Scn5a*, while ectopic Wnt GOF downregulates *Scn5a* and rescues the Notch-mediated effect (n=6 each genotype). Data are expressed as mean ± SEM. Group comparison in H was performed using a one-way ANOVA followed by a post-hoc Tukey's test. *p<0.05.

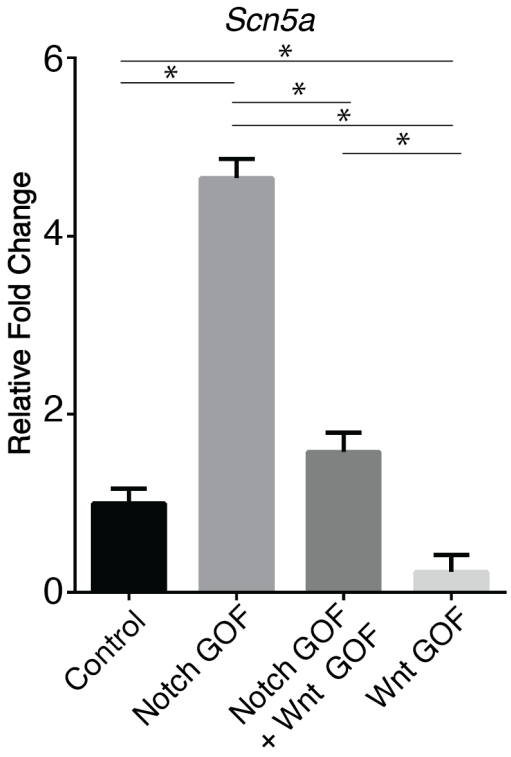

Several important questions remain unanswered. Firstly, what is the difference between those mice that undergo a complete and those that don't? Presumably, there are other cofactors that may affect the penetrance of the rescue. Morever, why is upregulation of Wnt dominant to upregulation of Notch in regulating *Scn5a* expression? Does Notch upregulate *Scn5a* through down regulation of Wnt or does it do so independently? For example, it is possible that β-catenin binds proteins on the *Scn5a* promoter to inhibit transcription while NICD binds CSL on or near those sites to initiate transcription or that Notch transcriptional targets, and not the NICD upregulate *Scn5a*.

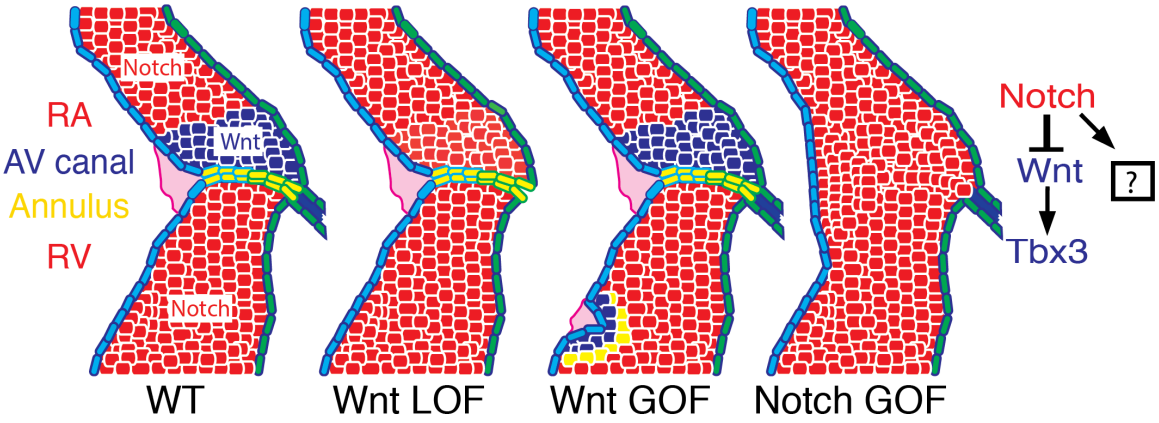

Figure 20. Model for Programming the AV Junction via Wnt and Notch
Notch signaling is active in the atria and ventricles (red) whereas canonical Wnt signaling (blue) is normally expressed in the AV junction during development (WT) and is required for maintenance of the AV myocardial phenotype and proper formation of the tricuspid valve (Wnt LOF). Ectopic Wnt activation within ventricular myocardium (Wnt GOF) is sufficient to induce *Tbx3* expression and ectopic AV junction properties as assessed by morphologic and electrical criteria. Ectopic Notch activation in postnatal AV junctional myocardium (Notch GOF) can globally reprogram gene expression in the AV junction, including inhibition of canonical Wnt signaling. Since Wnt LOF does not entirely phenocopy Notch GOF, Notch may additionally regulate other signaling pathways giving rise to ectopic myocardium.

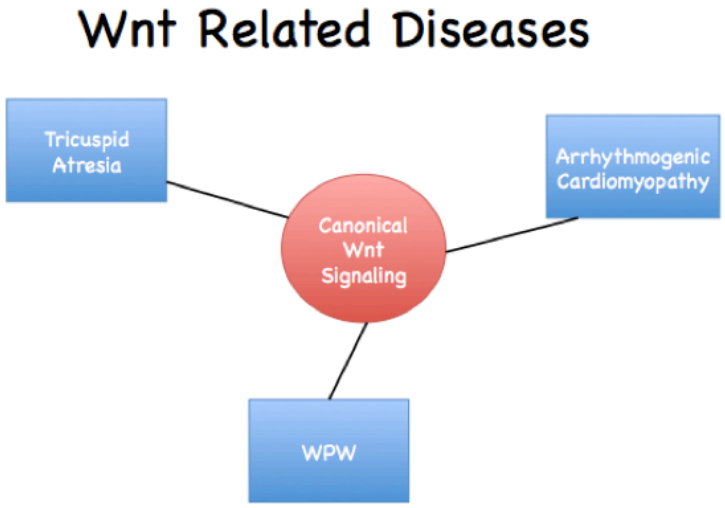

Figure 21. Wnt is involved in numerous mouse models of human disease.
Wnt LOF leads to tricuspid atresia (chapter 2). Wnt GOF leads to arrhythmogenic cardiomyopathy (chapter 3). While Wnt LOF does not lead to ventricular preexcitation, downregulation of canonical Wnt signaling is required for Notch induced ventricular preexcitation (chapter 4).

4.5 Contributions

ECGs were done by Stacey Rentschler, Stephanie Hicks, and Ben Gillers. Mouse breeding was done by Stephanie Hicks. Tissue was processed by Ben Gillers. *LacZ* and Trichrome staining

were done by Stephanie hicks and Ben Gillers. Immunostaining was done by Ben Gillers. qPCR was done by Aditi Chiplunkar and Ben Gillers.

Chapter 5: Gene Therapy In Vivo and In Vitro

5.1 Mouse Gene Painting in Vivo

The use of transgenic and knockin mice has been crucial for our understanding of development and disease. Indeed, the preceding data of this dissertation are derived from such mice. However, to rapidly test the affects of overexpression of different pathways requires other tools that do not involve development of new mouse models.

Viruses have long been used as vectors for gene delivery and present an excellent opportunity with which to screen signaling pathways in vivo. Furthermore, if we are to manipulate the signaling pathways described in this dissertation to treat human disease, we need an efficient delivery system that can be used in the context of human patients. Although gene therapy faced a major setback in 1999 due to the death of Jesse Gelsinger in a gene therapy clinical trial, much has been learned since then regarding the safety of this technology and gene therapy clinical trials are reemerging to treat a host of diseases [43, 73].

I therefore decided to expand on a gene therapy platform developed in recent years by Kevin Donehue's lab in pig and Mark Aderson's lab in mouse [74, 75]. Both have shown successful gene painting using a mixture of polymer, proteases, and virus applied on the atrial surface with a camel's hair paint brush. However, what is unclear with this system is how long the viral induced gene expression remains active in the atria. To test this, I made use of biolumisincent imaging (BLI). BLI can be used to monitor gene expression in a living animal [76, 77]. I used an Ad5 vector that contains the coding sequence for both GFP and firefly luciferase under the control of the CMV promoter. In the presence of D-luciferin, firefly luciferase catalyzes an enzymatic reaction

that produces light that can be captured with a high speed camera. This allows one to do a longitudal time course without having to sacrifice the animal mid-experiment. Presence of GFP allowed me to assess viral expression with single cell resolution; something not possible with in vivo BLI.

I found that while BLI signal peaked at 6 days, signal dramatically decreased by 2 weeks after gene painting (figure 22B,C). This decrease in signal may be due to clearance of the cells by the immune system. To directly test this hypothesis, I compared the persistence of adenoviral gene expression in control (Cd1) and immune compromised mice (NOD/SCID). The difference in BLI signal is striking. Already by 1 week, the signal in Cd1 beings to decrease while in NOD/SCID mice the signal continues to increase at 3 weeks (figure 22C). Importantly, when I sacrificed the mice and imaged GFP fluorescence I found signal only in the NOD/SCID hearts whereas I found no GFP in the Cd1 hearts. Furthermore, the LA in the Cd1 hearts was very unhealthy and covered in what is presumably an immune cell filled infiltrate. In the NOD/SCID mice, the RA and LA are both clearly discernable and healthy looking (figure 22D). Because GFP was not seen in the Cd1 hearts at 23 days, it is reasonable to assume that any gene activity in those mice was extraneous to the heart. Indeed, when I performed BLI after sacrificing the mice and opened the chest cavity, I detected small amounts of BLI on the chest wall but not on the actual heart. In NOD/SCID mice, I detected BLI on the LA in addition to the chest wall. In both groups, BLI was also detected in the liver.

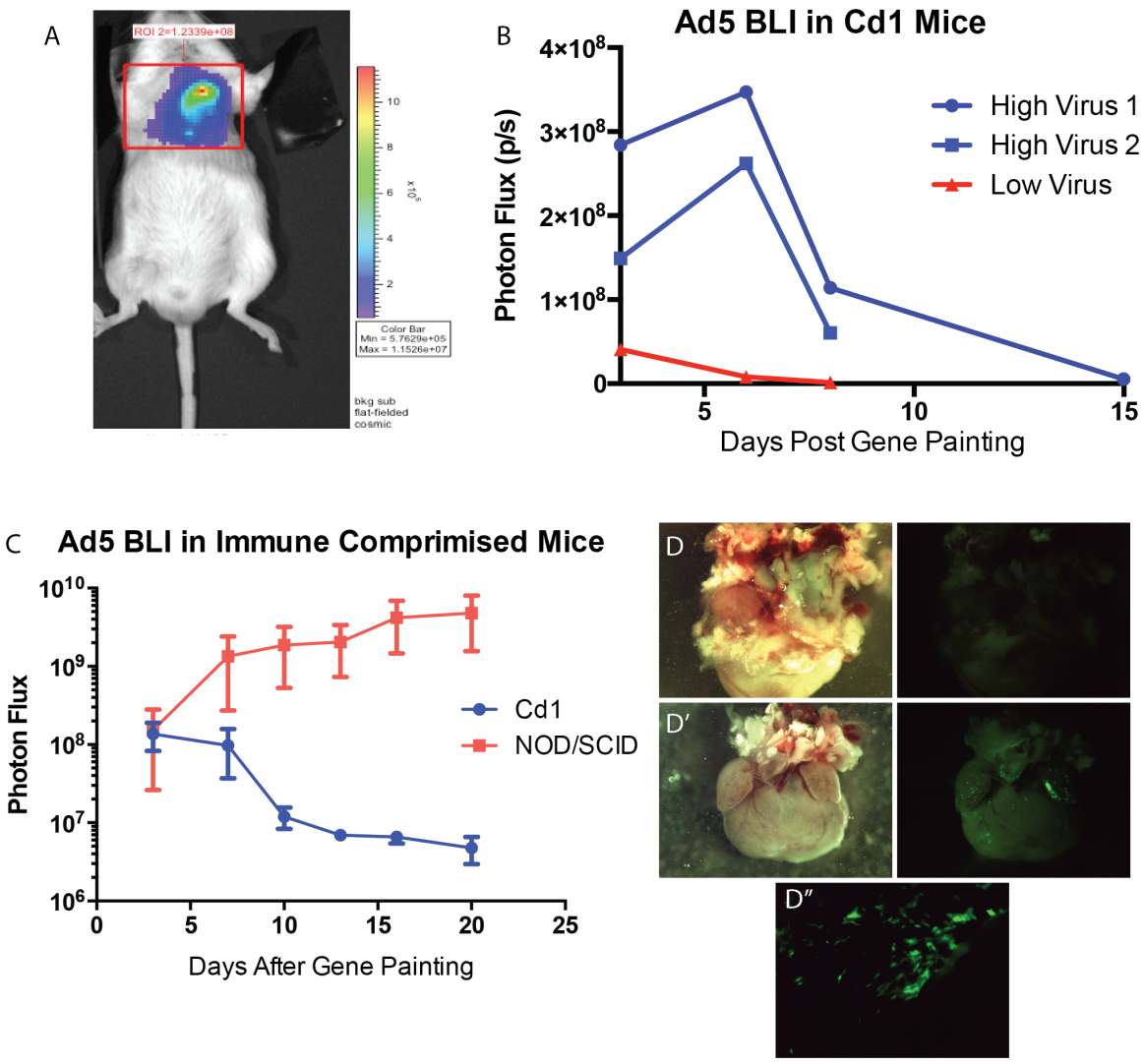

Figure 22. In vivo gene painting can be used for long term gene expression in NOD/SCID mice.
(A) In vivo bioluminescence image of a NOD/SCID mouse 3 days after gene painting. Signal is seen primarily in the chest cavity region, near the heart. (B) Bioluminescence comparison of virus volume in gene painting of Cd1 mice. Mice treated with high amount of virus (1.12x10^11 V.P.) peak in BLI signal at 6 days after gene painting while signal in the mouse treated with low amount of virus (1.40x10^10 V.P.)
peaks at day 3 and rapidly drops off by 6 days. (C) BLI comparison of expression of painted virus in NOD/SCID vs Cd1 mice. By 6 days, signal begins to decrease in Cd1 mice while in NOD/SCID mice, signal continues to increase even at 3 weeks. (D) Bright field and fluorescence imaging of gene painted hearts at 23 days post gene painting. In D, a Cd1 heart is shown with much immune infiltrate in the atrial region. While the RA is discernable, the LA is not. No fluorescence is seen in the Cd1 heart. (D') A NOD/SCID heart is shown with healthy looking atria and strong fluorescence seen in the LA. There is nominal fluorescence in the RA. (D'') Magnified image of GFP+ LA in D'. N=3 in C, D.

Eduardo Marban's group has shown that adenovirus expressing *Tbx18* can be injected into the porcine LV and induce an ectopic pacemaker site [78]. However, this effect was lost by 2 weeks

after injection. My data here strongly suggests that the immune system is responsible for this type of short lived effect. It is therefore imperative, when developing adenovirus based cardiac therapies, to use modified viruses that are capable of evading the immune system. It would be interesting to compare BLI signal using such a modified virus in a Cd1 mouse versus unmodified virus in a NOD/SCID mouse. I would expect that both would have similar long lasting gene expression.

5.2 Mouse Gene Painting in Vitro

Since in vivo gene painting requires a complicated surgery involving intubation and a thoracotomy, I wanted to be able to test different viruses in the heart in a more accessible fashion. To accomplish this, I used an atrial culture system used by the Efimov lab. I filleted open the atria and pinned it down; epicardial side facing up. When I initially painted polymer, I found that gene expression was seen throughout the tissue, even in regions that I did not paint polymer and virus. This is due to the fact that polaxymer 407 is hydro-soluble and therefore, dissolves in the solution after being painted on the cultured atria.

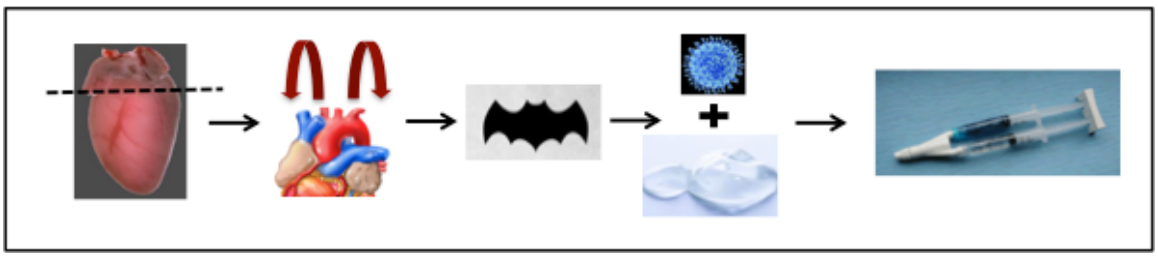

Figure 23. Schematic of in vitro painting protocol.
Atria are remove from the ventricles, filleted open, and painted with polymer/virus. Duraseal is then sprayed on to seal the polymer in place.

To circumvent this issue, I used a cap technology to seal the polymer onto the tissue. Once painted, I sealed the polymer using DuraSeal, a surgical adhesive used in spinal cord surgery.

Using this cap technology, the GFP expression became localized to the site of delivery (protocol illustrated in figure 23, data shown in figure 24).

Since the cost of DuraSeal is prohibitive, an alternative cap, such as a poly ethylene glycol (PEG) hydrogel may be worthwhile pursuing. Initial experiments with PEG diacrylate (PEGDA) illustrated the need for modifications since PEGDA fluoresced green under blue light, thereby preventing the monitoring of GFP fluorescence.

An alternative to the cap technology would be to abandon the use of polaxymer 407 in favor of a material that is not water-soluble. For example, a pellet of collagen mixed with virus could be gelled and placed on top of the tissue. Collagen has already been shown to be compatible in vivo with adenovirus and presents sustained delivery of the virus over time. An alternative is to use a microinjection system to directly inject virus without polymer into the tissue. Both of these methods have been successfully reported in the brain slice organotypic literature. Furthermore, collagen has been shown to be compatible with adenovirus and useful as a viral delivery vehicle in vivo [79].

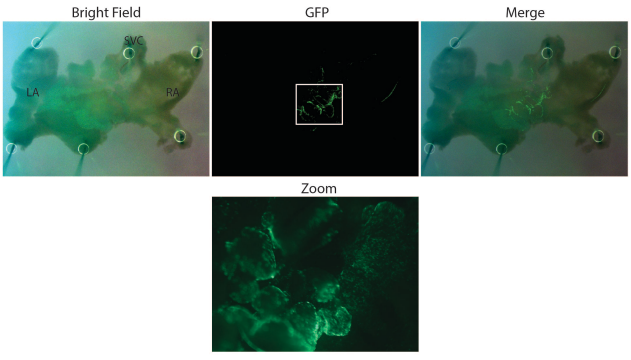

Figure 24. Localized gene expression after in vitro gene painting.
Mouse atria are filleted open and pinned down in a 6 well plate. GFP fluorescence is primarily seen, in this whole mount image, only in the middle of the tissue where virus/polymer was painted. Fluorescence lasts, at least until 6 days.

5.3 Human Cardiac Slices

Ultimately, one of the main goals of biomedical research is to develop therapies that can be used to treat human disease. Since we cannot do experiments on humans, we make do with model

organisms in which we can dissect the mechanisms of disease and test therapies. The major drawback to this approach is that humans are not identical to any model organism. In fact, many promising therapies that were proven efficacious and safe in animal studies were rejected in clinical trials due to unforeseen complications that arose only in humans and not in the preceding animal studies [80]. This highlights the need to validate a therapy in human tissue before bringing it to clinical trials. It would be highly advantageous to begin experiments with human tissue coincident with developing a therapy or dissecting a genetic pathway in mice. This would allow the human biology to directly inform the course of experiments in animal models.

To be able to do this, I began working with the human cardiac culture system published by Camelliti et al [81-83] and modified by the Efimov laboratory. It involves the use of a vibratome to slice hearts that were rejected for transplant. Based on the published literature, I began culturing these slices on transwells. This is to maintain the air-liquid interface and provide the tissue with maximal oxygen uptake. Initially, when I began working with the heart slices, I was only able to keep them alive for 1 day. After much trial and error, I found that it was crucial to fill the entire well, both in and out of the transwell with PBS each day to wash the tissue. Upon doing this, I have now been able to culture the slices reliably for up to 4 days. This requirement may be due to the high metabolism of myocytes. If the metabolic waste secreted by these cells is not washed out, it may be detrimental to the culture.

In order to study the effects of Wnt and Notch signaling in human cardiac tissue, I decided to develop a viral based gene delivery system within the human slice culture, similar to the system I developed with mouse atria.

When adding only GFP expressing virus (Ad5GFP), by 24 hours I found robust expression of GFP in punctate shaped cells (figure 25B). Upon immune staining with actinin, I found that only non-myocytes were GFP positive (figure 25E,F). I therefore decided to treat the tissue with protease to allow for deeper penetration of the virus into the tissue. Based on the published literature in mouse atria in vivo and my experiments in vitro, I initially mixed the virus with collagenase and trypsin. By 4 days in culture, myocytes became GFP positive in one heart. It is unclear why the myocytes take longer to express GFP than non-myocytes. Does it take longer for the viral particle to enter the myocyte or is the delay in the unpacking of the viral particle once inside the tissue or in the expression of GFP itself? Using viruses with different targeting modifications may help address this question.

Although this data is interesting, in remaining hearts, I could only detect GFP in non-myocytes. Furthermore, while trypsin and collagenase allowed for strong viral expression in one heart, I found that in remaining hearts, trypsin damages the human cardiac slices and actually prevents GFP expression (except in adipocytes where trypsin activity increases GFP expression). This may be due to a variation in the degree of health of different hearts from which we cut the human slices. I did find, however, that collagenase alone did not damage the tissue and increased GFP expression in the tissue.

Several important questions remain in this area of research. Firstly, can modifications of the viral particle not only decrease the time to GFP expression but also increase the targeting efficiency? Do certain modifications allow for higher myocyte uptake? Also, can a polymer base system be used to allow for spatial control of viral expression. Both the collagen droplet method and direct

micro injection are techniques worth investigating. It further remains to been what affects do collagenase treatment and viral expression have on the electrical properties of the tissue.

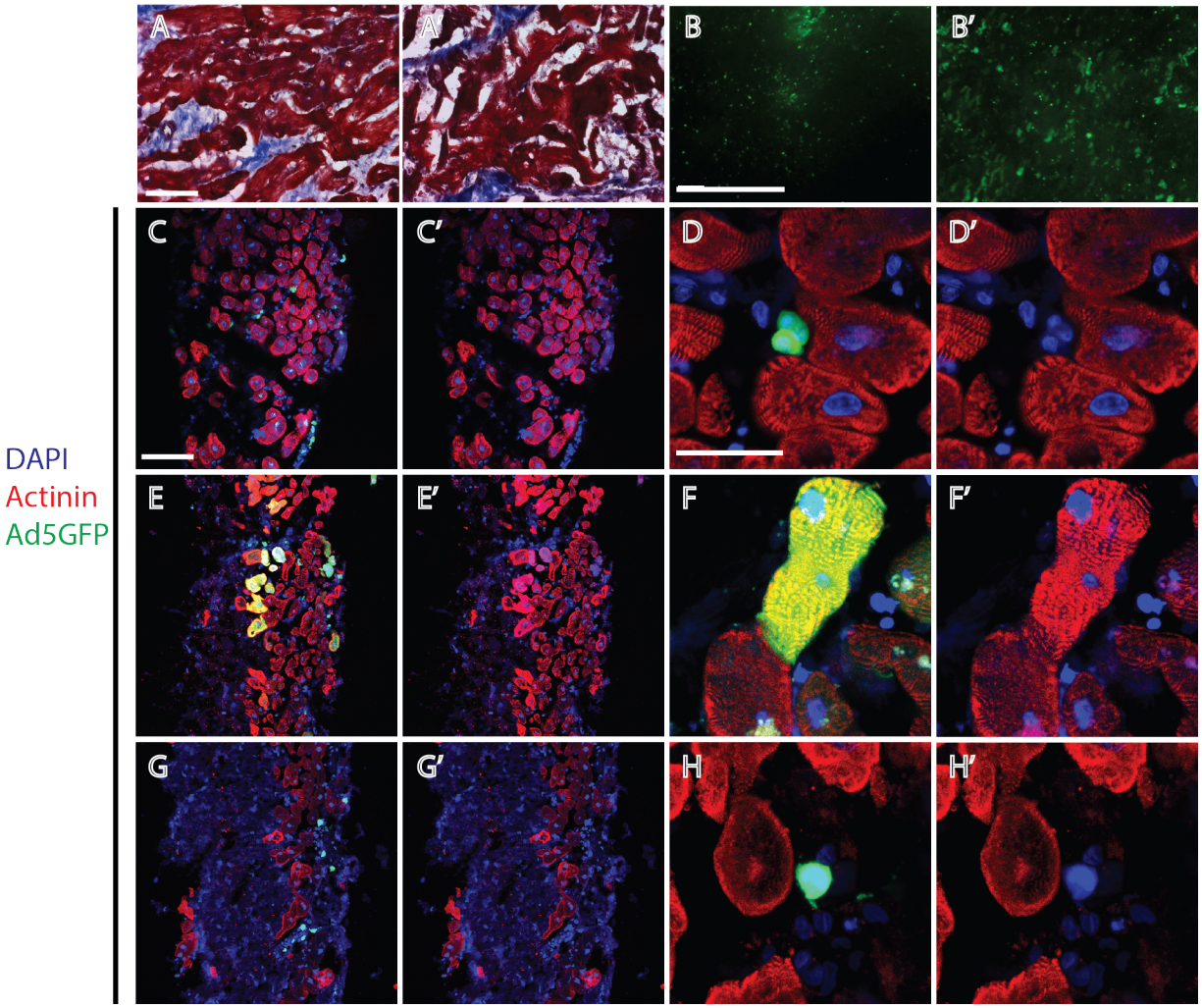

Figure 25. Organotypic slices from human donor hearts can be cultured and transduced with adenovirus. Donor hearts rejected for transplantation were sliced on a vibratome and cultured for 4 days. Trichrome of cardiac slice at 1 (A) and 4 days (A') in culture. Fibrotic regions can be seen in blue. (B) Whole mount GFP fluorescence at 1 (B) and 4 (B') days in culture in slices transduced with virus at D0. At 1 day, green punctate are seen. At 4 days, in 1 out of 10 hearts, large elongated cells are GFP+. (C-H) A transverse histological section of a cultured cardiac slice where the entire thickness of the cultured slice can be seen. (C) At 1 day in culture, GFP is seen only in small puncti, around the nucleus in non-myocytes. Myocytes are stained with actinin (red), nuclei with DAPI (blue). (C') is the same image as (C) without the green channel. (D) A zoomed in image of (C) where it is clear the GFP+ cell is not a myocyte. (D') The same image as (D) without the green channel. (E) At 4 days in culture, GFP can be seen in myocytes deep in the tissue. (E') The same image as (E) without the green channel. (F) A zoomed in image of (E) where GFP is clearly seen in the myocyte. (F') The same image as (F) without the green channel. The cell that is GFP+ in (F) is clearly actinin positive in (F'). (G) At 4 days in culture, GFP is primarily seen in non-myocytes. (G') The same image as (G) without the green channel. (H) A zoomed in image of (G) where GFP is seen in non-myocytes. (H') is the same image as (H) without the green channel. The cell that is GFP+ in (H) is clearly actinin negative in (H'). Scale bars are 100 μm except D where it is 50 μm.

5.4 Contributions

In vivo gene painting was done by Carla Weinheimer, Kalin Baechle, and Ben Gillers. BLI was performed by Julie Prior of the Optical Radiology Lab, Kailin Baechle, and Ben Gillers. Mouse in vitro gene painting was done by Jon Qiao and Ben Gillers. Hearts were brought from the operating room by Chaoyi Kang, Aditi Chiplunkar and Ben Gillers. Hearts were sliced by Chaoyi Kang, Jon Qiao, and Ben Gillers. Tissue was cultured and treated by Ben Gillers. Tissue was fixed and stained by Kailin Baechle and Ben Gillers. Images and figures were prepared by Ben Gillers.

Chapter 6: Methods

6.1 Mice

Mlc2v^{Cre} [19], *αMHC-Cre* [20], *αMHCrtTA*, *tetO-NICD* [29, 84], *Axin2*^{LacZ} [24], *Ctnnb1*^{fl} [28], *Ctnnb1*^{dm} [32, 84], *Ctnnb1*$^{fl(ex3)}$ [29], *NICD* [85], *Tbx2*^{Cre} [11] and *R26*^{TdTomato} [86] mice have been described previously, and were maintained on a mixed genetic background. For experiments involving conditional gene expression, timed pregnancies were determined and induction of gene expression was accomplished with doxycycline chow (BioServ 200 mg/kg) during the stated timepoints. *αMHCrtTA* and *tetO-NICD* littermates fed doxycycline were used for comparison in all conditional gene expression experiments unless otherwise noted. Littermate controls were used for all experiments. All animal protocols were approved by the Animal Studies Committee at Washington University

6.2 Histology and Immunohistochemistry

Immunohistochemistry was performed on paraffin-embedded and frozen sections with antibodies recognizing Tbx3 (sc-17871, Santa Cruz), connexin 40 (CX40-A, Alpha Diagnostic International), $Na_v1.5$ (AS-005, alomone labs), CD31 (DIA-310, dianova), and periostin (Ab14041, Abcam). Secondary antibody-fluorescent conjugates included anti-rabbit Alexa 568 (Invitrogen), anti-goat Alexa 488 (Invitrogen), and for connexin 40, signal amplification was performed using anti-rabbit ImmPRESS (MP-7401, Vector Laboratories) with TSA (SAT702001, Perkin Elmer). Histology, immunohistochemistry, and whole-mount Xgal images were analyzed using Adobe Photoshop. Control and mutant images were treated identically in all cases where brightness and contrast were altered.

6.3 In Situ Hybridization

In situ hybridization for *Bmp2* was performed as described previously. Digoxigenin-labeled probes were detected using an antidigoxigenin-alkaline phosphatase conjugate (Roche) and visualized with an enzyme catalyzed color reaction.

6.4 Reverse Transcription-Quantitative Polymerase Chain Reaction

Total RNA was isolated from atria/AV or ventricles using Trizol (Invitrogen) and DNase treated using TURBO DNA-*free* DNase Treatment Kit (Ambion). First-strand cDNA was synthesized using a high Capacity cDNA Reverse Transcription kit (Applied Biosystems). Gene expression was assayed using the Power SYBR Green PCR Master Mix (Applied Biosystems) with primers listed in the attached Table and quantified using the StepOne Plus Real-Time PCR system or ViiA™ 7 qRT-PCR systm (Applied Biosystems). Relative fold changes were calculated using the comparative threshold cycle methods ($2^{-\Delta\Delta Ct}$).

6.5 Optical Mapping

Optical mapping was performed as previously described [87]. Briefly, mice were anesthetized with a ketamine/xylazine cocktail (ketamine, 80 mg/kg bodyweight; xylazine, 10 mg/kg bodyweight) and heparinized (100 units) by intraperitoneal injection. Hearts were excised and mounted on a Langendorff set-up and perfused at 37°C with Tyrode's solution ((in mmol/L) 128.2 NaCl, 4.7 KCl, 1.19 Na H_2PO_4, 1.05 $MgCl_2$, 1.3 $CaCl_2$, 20.0 $NaHCO_3$, and 11.1 glucose, pH maintained at 7.4 by equilibration with a mixture of 95% O_2 and 5% CO_2). To record optical action potentials, a bolus injection of 10 mM Di-4-Anepps was administered with 15 mM blebbistatin to prevent motion artifacts. Optical signals were processed using MATLAB software. All optical signals were spatially binned (5x5 pixels), filtered using a 0-100Hz finite impulse response filter, and

normalized. Activation times were defined at dV_m/dt_{max}. Simultaneous recording of a pseudo-electrocardiogram using electrograms placed 5 mm from the heart was performed, and the QRS duration was determined according to previously described methodology [88].

6.6 In vivo Gene Painting and Bioluminescent Imaging

Adeno virus was mixed with polaxymer 407 and trypsin and collagenase. The polaxymer allows the mixture to adhere to the atria while the trypsin and collagenase allow viral penetration into the myocardium. The mixture was prepared the day before surgery to allow for proper solubilization of the polymer.

Cd1 or NOD/SCID mice were placed under anesthesia and intubated. They underwent a thoracotomy and a the virus/polymer mixture was painted on the LA. The chest was left open for 5 minutes to allow penetration of the virus and proteases. A 2nd round of painting was done followed by another 5 minute wait. The chest cavity was sutured and mice were imaged starting 3 days after surgery.

D-Luciferin was injected intraperatonealy and mice were left while conscious for 5 minutes to allow for distribution of D-Luciferin. Mice were then placed under isoflurane for 5 minutes and imaged with a high-speed camera for 1 to 60 seconds. The injected virus contains the firefly luciferase gene that catalyzes a light emitting enzymatic reaction in the presence of D-Luciferin. Therefore, this technique can be used to detect active gene expression in vivo.

6.7 In Vitro Mouse Gene Painting

The virus/polymer mixture used for in vivo painting was used for in vitro painting of the mouse atria. Mice were sacrificed and their hearts were perfused on a Langendorf perfusion with Krebbs solution at 37 C. The atria were removed and dissected open and pinned down in a 6 well plate, epicardium facing up. Virus was painted on the atria. The painted region was then coated with DuraSeal and placed in a tissue culture incubator. Medium was changed every day for 6 days.

6.8 In Vitro Human Cardiac Slice Culture

Human hearts that were rejected for transplantation were perfused with cardioplegia and collected by a cardiothoracic surgeon. Hearts were transported to the laboratory in ice cold cardioplegia. A piece of the LV free wall was placed in ice cold tyrodes solution and sliced on a vibratome in 380 uM sections and an advance rate of 4um/s. Slices were cultured on trasnwells in M199 media with 1% Insulin/Transferin/Selenium and penicillin/streptomycin. Slices were treated with 15 uL protease and virus and left on the tissue over night. Slices were washed in PBS every day.

6.9 Statistical Analysis

All data are expressed as means ± standard error (SEM). Statistical analyses were performed using student unpaired *t* tests or one-way ANOVA followed by post-hoc Tukey's test. Significant differences are indicated by $*P<0.05$, $**P<0.005$.

Chapter 7: Conclusion

I have presented here a model where Notch and Wnt signaling program distinct cardiac regions. While Wnt signaling programs a junction/nodal phenotype, Notch signaling programs working myocardium and limits the activity of Wnt activation. Several important questions remain in further developing this model.

7.1 What Regulates the Notch/Wnt Balance?

I have posited that Wnt activation is limited primarily to nodal tissue as a result of Notch activation in non-nodal tissue. This model places Notch signaling upstream of Wnt signaling. What is upstream of Notch signaling? Why is it not active in the AVC myocardium? Is there an inhibitory signal in the presumptive AVC which prevents active Notch signaling? Does Wnt signaling in the AVC inhibit Notch signaling? If so, why is Wnt's inhibition of Notch dominant in the AVC but vice versa in working myocardium? Presumably, there are cofactors which regulate these two aspects of regional cardiac specification. What are those factors and how do the interact with the proposed signaling pathway?

Another intriguing questions lies in the stochasticity of ectopic AVJs. I have shown, based on several criteria, that Wnt activation programs ectopic AVJs. However, these fibrofatty depositions appear at seemingly random sites in the ventricles. They can be at the apex or they can be more lateral. Furthermore, there doesn't appear to be a set number of these foci. In addition, in the embryo, the ectopic Tbx3/perisotin pattern can also emerge in varying regions; whether at the apex of the LV or as an expansion of the AV canal/nodal region. What determines where these foci develop?

One may be tempted to explain this based on the spottiness of *Mlc2v*^{Cre} expression. However, as noted earlier, *αMHC-Cre* is expressed ubiquitously throughout the heart and even when using that Cre to over activate canonical Wnt singling, the ectopic Tbx3 expression is also stochastic in its spatial distribution. Therefore, the choice of tools in this experiment does not explain the random distribution.

There are two interesting mechanisms that may explain this phenomena. As mentioned earlier, Notch signaling is active in the ventricles. In particular, *Hey2* is expressed in the ventricles while *Hey1* is expressed in the atria [41]. There may exist different levels of *Hey2* expression throughout the ventricles. As I have shown earlier, Notch signaling downregulates the activity of canonical Wnt signaling. Therefore, it is possible, that regions of the ventricles which have low(er) Notch activity are susceptible to Wnt induced overexpression whereas regions with higher endogenous Notch activity are not susceptible since their Notch activity may prevent those regions from becoming programmed by ectopic Wnt activation.

This hypothesis may also explain why Wnt GOF completely rescues Notch induced preexcitation in 25% of mice. It is possible that in the 75% of mice that are not completely rescued, there is a higher level of endogenous Notch activation that prevents Wnt activation from being able to rescue the phenotype. In the remaining 25% of mice that are completely rescued, there may be lower endogenous Notch activation and therefore these mice can be rescued by Wnt activation.

Bmp2 signaling may present an alternative mechanism in understanding the stochastic nature of the ectopic AV junctions. Bmp2 signaling, primarily expressed in the AVC, is required for

development of that tissue [35]. However, it is also expressed at low levels in the ventricles. It is possible that Wnt signaling is able to specify an ecptoic AVJ only in regions that already have a threshold level of *Bmp2* which makes them "pre-specified" and permissive to Wnt's specification. Being that the direct Notch target, *Hey2* has been shown to limit Bmp2 expression primarily to the AVC, small amounts of *Bmp2* expression in the ventricle may be the result of lower Notch activation. Therefore, this hypothesis may in fact be a further iteration of my previously described Notch hypothesis as apposed to a completely independent mechanism.

7.2 How Does Notch Inhibit Wnt Signaling?

Another area of speculation lies in Notch's inhibition of Wnt singling. As mentioned earlier, Kwon et al posited that in Isl1 myocyte progenitors, NICD targets β-catenin for lysosomal degradation [72]. Although this mechanism may be true in myocyte progenitors, there are several other hypotheses to take into consideration in AVC myocytes. The mechanism does not lie in regulation of *β-catenin* transcript levels since in Notch activated mice, *β-catenin* transcript levels remain unchanged. This suggest that the mechanism is post transcriptional, either in regulating β-catenin protein levels or activity. Notch signaling may prevent translation of the *β-catenin* message. This would lead to lower β-catenin levels and hence lower Wnt activation. An alternative explanation is that although initially β-catenin protein levels are the same, they are either prevented from enter the nucleus or from activating downstream transcription once in the nucleus. This would likely occur through a post translational modification which would affect its nuclear localization signal from targeting it to the nucleus. Alternatively, once β-catenin enters the nucleus, it cannot bind target sites due to either sequestration of β-catenin in the nucleus or occupation of TCF/LEF binding sites by competitor proteins.

On a similar note, what aspect of Notch signaling inhibits Wnt activity? Is it NICD itself participating in competitive binding or sequestration or are Notch downstream effectors (such a Hey1 or Hey2) required for this inhibition. It would be interesting to assess Wnt activity in a *Hey1* or *Hey2* overexpression mouse that would activate Notch downstream effectors without over activating the NICD.

7.3 What Causes Specific Right Sided Phenotypes?

Another are of interest is the right sided nature of several phenotypes presented here. The Notch induced accessory pathways are primarily right sided. The Wnt GOF induced inexcitability was predominant in the RV. Lastly, in the Wnt LOF, the tricuspid, and not mitral, valve is atretic. This suggests that there may be a certain program that regulates the right versus left side of the heart. It is important to realize that the right sided nature of these three phenotypes may all be dependent on different mechanisms. For example, the longer refractory period in the Wnt GOF may be dependent on expression of different ion channels in the RV versus the LV which make it more susceptible to a prolonged refractory period. Indeed, the effects of adult Wnt activation in the atria was different for the RA and LA in downregulating *Scn5a*. The atretic tricuspid valve is likely not due to ion channel expression but possibly a result of a specific genetic network which programs the right vs left side of the AVC. For example, Tbx3, which is regulated by Wnt signaling, is primarily a right sided factor whereas Tbx2 is more highly expressed in the left side of the AVC. This leads to the intriguing possibility that the right side of the heart is regulated by a Wnt-Tbx3 axis and left side of the AVC is regulated by a Tbx2 dependent pathway. The right sided accessory pathways may also be dependent on this differential program.

The role of Notch and Wnt presented here, and their interplay provide a deeper understanding of the signaling pathways that program distinct regions of the heart. Furthermore, understanding how perturbation of these pathways leads to disease may give us a better direction for developing targeted therapies. The use of gene therapy may provide a useful platform for targeting these pathways in the treatment of disease.

References

1. Rentschler S, Morley GE, Fishman GI. Molecular and functional maturation of the murine cardiac conduction system. *Cold Spring Harb Symp Quant Biol.* 2002;67:353-361.

2. Hahurij ND, Gittenberger-De Groot AC, Kolditz DP, Bokenkamp R, Schalij MJ, Poelmann RE, Blom NA. Accessory atrioventricular myocardial connections in the developing human heart: relevance for perinatal supraventricular tachycardias. *Circulation.* 2008;117(22):2850-2858.

3. de Lange FJ, Moorman AF, Anderson RH, Manner J, Soufan AT, de Gier-de Vries C, Schneider MD, Webb S, van den Hoff MJ, Christoffels VM. Lineage and morphogenetic analysis of the cardiac valves. *Circ Res.* 2004;95(6):645-654.

4. Boukens BJ, Rivaud MR, Rentschler S, Coronel R. Misinterpretation of the mouse ECG: 'musing the waves of Mus musculus'. *J Physiol.* 2014;592(Pt 21):4613-4626.

5. Wakker V, Brons JF, Aanhaanen WT, van Roon MA, Moorman AF, Christoffels VM. Generation of mice with a conditional null allele for Tbx2. *Genesis.*48(3):195-199.

6. Chapman DL, Garvey N, Hancock S, Alexiou M, Agulnik SI, Gibson-Brown JJ, Cebra-Thomas J, Bollag RJ, Silver LM, Papaioannou VE. Expression of the T-box family genes, Tbx1-Tbx5, during early mouse development. *Dev Dyn.* 1996;206(4):379-390.

7. Christoffels VM, Hoogaars WM, Tessari A, Clout DE, Moorman AF, Campione M. T-box transcription factor Tbx2 represses differentiation and formation of the cardiac chambers. *Dev Dyn.* 2004;229(4):763-770.

8. Harrelson Z, Kelly RG, Goldin SN, Gibson-Brown JJ, Bollag RJ, Silver LM, Papaioannou VE. Tbx2 is essential for patterning the atrioventricular canal and for morphogenesis of the outflow tract during heart development. *Development.* 2004;131(20):5041-5052.

9. Harrelson Z, Papaioannou VE. Segmental expression of the T-box transcription factor, Tbx2, during early somitogenesis. *Dev Dyn.* 2006;235(11):3080-3084.

10. Bakker ML, Boukens BJ, Mommersteeg MT, Brons JF, Wakker V, Moorman AF, Christoffels VM. Transcription factor Tbx3 is required for the specification of the atrioventricular conduction system. *Circ Res.* 2008;102(11):1340-1349.

11. Aanhaanen WT, Brons JF, Dominguez JN, Rana MS, Norden J, Airik R, Wakker V, de Gier-de Vries C, Brown NA, Kispert A, Moorman AF, Christoffels VM. The Tbx2+ primary myocardium of the atrioventricular canal forms the atrioventricular node and the base of the left ventricle. *Circ Res.* 2009;104(11):1267-1274.

12. Singh R, Horsthuis T, Farin HF, Grieskamp T, Norden J, Petry M, Wakker V, Moorman AF, Christoffels VM, Kispert A. Tbx20 interacts with smads to confine tbx2 expression to the atrioventricular canal. *Circ Res.* 2009;105(5):442-452.

13. Goudevenos JA, Katsouras CS, Graekas G, Argiri O, Giogiakas V, Sideris DA. Ventricular pre-excitation in the general population: a study on the mode of presentation and clinical course. *Heart.* 2000;83(1):29-34.

14. Boukens BJ, Janse MJ. Brief history of arrhythmia in the WPW syndrome - the contribution of George Ralph Mines. *J Physiol.* 2013;591(Pt 17):4067-4071.

15. Sidhu JS, Rajawat YS, Rami TG, Gollob MH, Wang Z, Yuan R, Marian AJ, DeMayo FJ, Weilbacher D, Taffet GE, Davies JK, Carling D, Khoury DS, Roberts R. Transgenic mouse model of ventricular preexcitation and atrioventricular reentrant tachycardia induced by an AMP-activated protein kinase loss-of-function mutation responsible for Wolff-Parkinson-White syndrome. *Circulation.* 2005;111(1):21-29.

16. Patel VV, Arad M, Moskowitz IP, Maguire CT, Branco D, Seidman JG, Seidman CE, Berul CI. Electrophysiologic characterization and postnatal development of ventricular pre-excitation in a mouse model of cardiac hypertrophy and Wolff-Parkinson-White syndrome. *J Am Coll Cardiol.* 2003;42(5):942-951.

17. Aanhaanen WT, Boukens BJ, Sizarov A, Wakker V, de Gier-de Vries C, van Ginneken AC, Moorman AF, Coronel R, Christoffels VM. Defective Tbx2-dependent patterning of the atrioventricular canal myocardium causes accessory pathway formation in mice. *J Clin Invest.* 2011;121(2):534-544.

18. Rentschler S, Harris BS, Kuznekoff L, Jain R, Manderfield L, Lu MM, Morley GE, Patel VV, Epstein JA. Notch signaling regulates murine atrioventricular conduction and the formation of accessory pathways. *J Clin Invest.* 2011;121(2):525-533.

19. Chen J, Kubalak SW, Chien KR. Ventricular muscle-restricted targeting of the RXRalpha gene reveals a non-cell-autonomous requirement in cardiac chamber morphogenesis. *Development.* 1998;125(10):1943-1949.

20. Agah R, Frenkel PA, French BA, Michael LH, Overbeek PA, Schneider MD. Gene recombination in postmitotic cells. Targeted expression of Cre recombinase provokes cardiac-restricted, site-specific rearrangement in adult ventricular muscle in vivo. *J Clin Invest.* 1997;100(1):169-179.

21. Ai D, Fu X, Wang J, Lu MF, Chen L, Baldini A, Klein WH, Martin JF. Canonical Wnt signaling functions in second heart field to promote right ventricular growth. *Proc Natl Acad Sci U S A.* 2007;104(22):9319-9324.

22. Cohen ED, Wang Z, Lepore JJ, Lu MM, Taketo MM, Epstein DJ, Morrisey EE. Wnt/beta-catenin signaling promotes expansion of Isl-1-positive cardiac progenitor cells through regulation of FGF signaling. *J Clin Invest.* 2007;117(7):1794-1804.

23. Kwon C, Arnold J, Hsiao EC, Taketo MM, Conklin BR, Srivastava D. Canonical Wnt signaling is a positive regulator of mammalian cardiac progenitors. *Proc Natl Acad Sci U S A.* 2007;104(26):10894-10899.

24. Lustig B, Jerchow B, Sachs M, Weiler S, Pietsch T, Karsten U, van de Wetering M, Clevers H, Schlag PM, Birchmeier W, Behrens J. Negative feedback loop of Wnt signaling through upregulation of conductin/axin2 in colorectal and liver tumors. *Mol Cell Biol.* 2002;22(4):1184-1193.

25. Barolo S. Transgenic Wnt/TCF pathway reporters: all you need is Lef? *Oncogene.* 2006;25(57):7505-7511.

26. Fancy SP, Harrington EP, Yuen TJ, Silbereis JC, Zhao C, Baranzini SE, Bruce CC, Otero JJ, Huang EJ, Nusse R, Franklin RJ, Rowitch DH. Axin2 as regulatory and therapeutic target in newborn brain injury and remyelination. *Nat Neurosci.* 2011;14(8):1009-1016.

27. Baba Y, Garrett KP, Kincade PW. Constitutively active beta-catenin confers multilineage differentiation potential on lymphoid and myeloid progenitors. *Immunity.* 2005;23(6):599-609.

28. Brault V, Moore R, Kutsch S, Ishibashi M, Rowitch DH, McMahon AP, Sommer L, Boussadia O, Kemler R. Inactivation of the beta-catenin gene by Wnt1-Cre-mediated deletion results in dramatic brain malformation and failure of craniofacial development. *Development.* 2001;128(8):1253-1264.

29. Harada N, Tamai Y, Ishikawa T, Sauer B, Takaku K, Oshima M, Taketo MM. Intestinal polyposis in mice with a dominant stable mutation of the beta-catenin gene. *EMBO J.* 1999;18(21):5931-5942.

30. Garcia-Gras E, Lombardi R, Giocondo MJ, Willerson JT, Schneider MD, Khoury DS, Marian AJ. Suppression of canonical Wnt/beta-catenin signaling by nuclear plakoglobin recapitulates phenotype of arrhythmogenic right ventricular cardiomyopathy. *J Clin Invest.* 2006;116(7):2012-2021.

31. Li J, Swope D, Raess N, Cheng L, Muller EJ, Radice GL. Cardiac tissue-restricted deletion of plakoglobin results in progressive cardiomyopathy and activation of {beta}-catenin signaling. *Mol Cell Biol.* 2011;31(6):1134-1144.

32. Valenta T, Gay M, Steiner S, Draganova K, Zemke M, Hoffmans R, Cinelli P, Aguet M, Sommer L, Basler K. Probing transcription-specific outputs of beta-catenin in vivo. *Genes Dev.* 2011;25(24):2631-2643.

33. Tian Y, Cohen ED, Morrisey EE. The importance of Wnt signaling in cardiovascular development. *Pediatr Cardiol.* 2010;31(3):342-348.

34. Grigoryan T, Wend P, Klaus A, Birchmeier W. Deciphering the function of canonical Wnt signals in development and disease: conditional loss- and gain-of-function mutations of beta-catenin in mice. *Genes Dev.* 2008;22(17):2308-2341.

35. Verhoeven MC, Haase C, Christoffels VM, Weidinger G, Bakkers J. Wnt signaling regulates atrioventricular canal formation upstream of BMP and Tbx2. *Birth Defects Res A Clin Mol Teratol.* 2011;91(6):435-440.

36. Tian Y, Yuan L, Goss AM, Wang T, Yang J, Lepore JJ, Zhou D, Schwartz RJ, Patel V, Cohen ED, Morrisey EE. Characterization and in vivo pharmacological rescue of a Wnt2-Gata6 pathway required for cardiac inflow tract development. *Dev Cell.* 2010;18(2):275-287.

37. Tung JJ, Tattersall IW, Kitajewski J. Tips, stalks, tubes: notch-mediated cell fate determination and mechanisms of tubulogenesis during angiogenesis. *Cold Spring Harb Perspect Med.* 2012;2(2):a006601.

38. Zine A, Van De Water TR, de Ribaupierre F. Notch signaling regulates the pattern of auditory hair cell differentiation in mammals. *Development.* 2000;127(15):3373-3383.

39. Manderfield LJ, High FA, Engleka KA, Liu F, Li L, Rentschler S, Epstein JA. Notch activation of Jagged1 contributes to the assembly of the arterial wall. *Circulation.* 2012;125(2):314-323.

40. Rizzo P, Mele D, Caliceti C, Pannella M, Fortini C, Clementz AG, Morelli MB, Aquila G, Ameri P, Ferrari R. The role of notch in the cardiovascular system: potential adverse effects of investigational notch inhibitors. *Front Oncol.* 2014;4:384.

41. Kokubo H, Tomita-Miyagawa S, Hamada Y, Saga Y. Hesr1 and Hesr2 regulate atrioventricular boundary formation in the developing heart through the repression of Tbx2. *Development.* 2007;134(4):747-755.

42. Luna-Zurita L, Prados B, Grego-Bessa J, Luxan G, del Monte G, Benguria A, Adams RH, Perez-Pomares JM, de la Pompa JL. Integration of a Notch-dependent mesenchymal

gene program and Bmp2-driven cell invasiveness regulates murine cardiac valve formation. *J Clin Invest.*120(10):3493-3507.

43. Yarborough M, Sharp RR. Public trust and research a decade later: what have we learned since Jesse Gelsinger's death? *Mol Genet Metab.* 2009;97(1):4-5.

44. Bongianino R, Priori SG. Gene therapy to treat cardiac arrhythmias. *Nat Rev Cardiol.* 2015.

45. Hanna J, Wernig M, Markoulaki S, Sun CW, Meissner A, Cassady JP, Beard C, Brambrink T, Wu LC, Townes TM, Jaenisch R. Treatment of sickle cell anemia mouse model with iPS cells generated from autologous skin. *Science.* 2007;318(5858):1920-1923.

46. Sauer AV, Di Lorenzo B, Carriglio N, Aiuti A. Progress in gene therapy for primary immunodeficiencies using lentiviral vectors. *Curr Opin Allergy Clin Immunol.* 2014;14(6):527-534.

47. Luo J, Luo Y, Sun J, Zhou Y, Zhang Y, Yang X. Adeno-associated virus-mediated cancer gene therapy: current status. *Cancer Lett.* 2015;356(2 Pt B):347-356.

48. Alba R, Bosch A, Chillon M. Gutless adenovirus: last-generation adenovirus for gene therapy. *Gene Ther.* 2005;12 Suppl 1:S18-27.

49. Ravens U. Antiarrhythmic therapy in atrial fibrillation. *Pharmacol Ther.* 2010;128(1):129-145.

50. Chiplunkar AR, Lung TK, Alhashem Y, Koppenhaver BA, Salloum FN, Kukreja RC, Haar JL, Lloyd JA. Kruppel-like factor 2 is required for normal mouse cardiac development. *PLoS One.* 2013;8(2):e54891.

51. Horsthuis T, Buermans HP, Brons JF, Verkerk AO, Bakker ML, Wakker V, Clout DE, Moorman AF, t Hoen PA, Christoffels VM. Gene expression profiling of the forming atrioventricular node using a novel tbx3-based node-specific transgenic reporter. *Circ Res.* 2009;105(1):61-69.

52. Cai X, Nomura-Kitabayashi A, Cai W, Yan J, Christoffels VM, Cai CL. Myocardial Tbx20 regulates early atrioventricular canal formation and endocardial epithelial-mesenchymal transition via Bmp2. *Dev Biol.* 2011;360(2):381-390.

53. Lie-Venema H, Eralp I, Markwald RR, van den Akker NM, Wijffels MC, Kolditz DP, van der Laarse A, Schalij MJ, Poelmann RE, Bogers AJ, Gittenberger-de Groot AC. Periostin expression by epicardium-derived cells is involved in the development of the atrioventricular valves and fibrous heart skeleton. *Differentiation.* 2008;76(7):809-819.

54. Kolditz DP, Wijffels MC, Blom NA, van der Laarse A, Hahurij ND, Lie-Venema H, Markwald RR, Poelmann RE, Schalij MJ, Gittenberger-de Groot AC. Epicardium-derived cells in development of annulus fibrosis and persistence of accessory pathways. *Circulation.* 2008;117(12):1508-1517.

55. Jansen JA, van Veen TA, de Bakker JM, van Rijen HV. Cardiac connexins and impulse propagation. *J Mol Cell Cardiol.*48(1):76-82.

56. Leaf DE, Feig JE, Vasquez C, Riva PL, Yu C, Lader JM, Kontogeorgis A, Baron EL, Peters NS, Fisher EA, Gutstein DE, Morley GE. Connexin40 imparts conduction heterogeneity to atrial tissue. *Circ Res.* 2008;103(9):1001-1008.

57. Bressan M, Liu G, Mikawa T. Early mesodermal cues assign avian cardiac pacemaker fate potential in a tertiary heart field. *Science.* 2013;340(6133):744-748.

58. Taathes DJ. *Cell Imaging Techniques: Methods and Protocols*: Humana Press; 2006.

59. Bezzina CR, Barc J, Mizusawa Y, Remme CA, Gourraud JB, Simonet F, Verkerk AO, Schwartz PJ, Crotti L, Dagradi F, Guicheney P, Fressart V, Leenhardt A, Antzelevitch C, Bartkowiak S, Borggrefe M, Schimpf R, Schulze-Bahr E, Zumhagen S, Behr ER, Bastiaenen R, Tfelt-Hansen J, Olesen MS, Kaab S, Beckmann BM, Weeke P, Watanabe H, Endo N, Minamino T, Horie M, Ohno S, Hasegawa K, Makita N, Nogami A, Shimizu W, Aiba T, Froguel P, Balkau B, Lantieri O, Torchio M, Wiese C, Weber D, Wolswinkel R, Coronel R, Boukens BJ, Bezieau S, Charpentier E, Chatel S, Despres A, Gros F, Kyndt F, Lecointe S, Lindenbaum P, Portero V, Violleau J, Gessler M, Tan HL, Roden DM, Christoffels VM, Le Marec H, Wilde AA, Probst V, Schott JJ, Dina C, Redon R. Common variants at SCN5A-SCN10A and HEY2 are associated with Brugada syndrome, a rare disease with high risk of sudden cardiac death. *Nat Genet.* 2013;45(9):1044-1049.

60. Gittenberger-de Groot AC, Vrancken Peeters MP, Mentink MM, Gourdie RG, Poelmann RE. Epicardium-derived cells contribute a novel population to the myocardial wall and the atrioventricular cushions. *Circ Res.* 1998;82(10):1043-1052.

61. Dettman RW, Denetclaw W, Jr., Ordahl CP, Bristow J. Common epicardial origin of coronary vascular smooth muscle, perivascular fibroblasts, and intermyocardial fibroblasts in the avian heart. *Dev Biol.* 1998;193(2):169-181.

62. Stroud DM, Gaussin V, Burch JB, Yu C, Mishina Y, Schneider MD, Fishman GI, Morley GE. Abnormal conduction and morphology in the atrioventricular node of mice with atrioventricular canal targeted deletion of Alk3/Bmpr1a receptor. *Circulation.* 2007;116(22):2535-2543.

63. Mahtab EA, Gittenberger-de Groot AC, Vicente-Steijn R, Lie-Venema H, Rijlaarsdam ME, Hazekamp MG, Bartelings MM. Disturbed myocardial connexin 43 and N-cadherin expressions in hypoplastic left heart syndrome and borderline left ventricle. *J Thorac Cardiovasc Surg.* 2012;144(6):1315-1322.

64. King JH, Huang CL, Fraser JA. Determinants of myocardial conduction velocity: implications for arrhythmogenesis. *Front Physiol.* 2013;4:154.

65. Bakker ML, Boink GJ, Boukens BJ, Verkerk AO, van den Boogaard M, den Haan AD, Hoogaars WM, Buermans HP, de Bakker JM, Seppen J, Tan HL, Moorman AF, t Hoen PA, Christoffels VM. T-box transcription factor TBX3 reprogrammes mature cardiac myocytes into pacemaker-like cells. *Cardiovasc Res.* 2012;94(3):439-449.

66. Hoogaars WM, Engel A, Brons JF, Verkerk AO, de Lange FJ, Wong LY, Bakker ML, Clout DE, Wakker V, Barnett P, Ravesloot JH, Moorman AF, Verheijck EE, Christoffels VM. Tbx3 controls the sinoatrial node gene program and imposes pacemaker function on the atria. *Genes Dev.* 2007;21(9):1098-1112.

67. Bateson P, Barker D, Clutton-Brock T, Deb D, D'Udine B, Foley RA, Gluckman P, Godfrey K, Kirkwood T, Lahr MM, McNamara J, Metcalfe NB, Monaghan P, Spencer HG, Sultan SE. Developmental plasticity and human health. *Nature.* 2004;430(6998):419-421.

68. Tabibiazar R, Wagner RA, Liao A, Quertermous T. Transcriptional profiling of the heart reveals chamber-specific gene expression patterns. *Circ Res.* 2003;93(12):1193-1201.

69. Christoffels VM, Smits GJ, Kispert A, Moorman AF. Development of the pacemaker tissues of the heart. *Circ Res.* 2010;106(2):240-254.

70. Chen SN, Gurha P, Lombardi R, Ruggiero A, Willerson JT, Marian AJ. The hippo pathway is activated and is a causal mechanism for adipogenesis in arrhythmogenic cardiomyopathy. *Circ Res.* 2014;114(3):454-468.
71. Rutenberg JB, Fischer A, Jia H, Gessler M, Zhong TP, Mercola M. Developmental patterning of the cardiac atrioventricular canal by Notch and Hairy-related transcription factors. *Development.* 2006;133(21):4381-4390.
72. Kwon C, Cheng P, King IN, Andersen P, Shenje L, Nigam V, Srivastava D. Notch post-translationally regulates beta-catenin protein in stem and progenitor cells. *Nat Cell Biol.* 2011;13(10):1244-1251.
73. Greener I, Donahue JK. Gene therapy strategies for cardiac electrical dysfunction. *J Mol Cell Cardiol.* 2011;50(5):759-765.
74. Swaminathan PD, Purohit A, Soni S, Voigt N, Singh MV, Glukhov AV, Gao Z, He BJ, Luczak ED, Joiner ML, Kutschke W, Yang J, Donahue JK, Weiss RM, Grumbach IM, Ogawa M, Chen PS, Efimov I, Dobrev D, Mohler PJ, Hund TJ, Anderson ME. Oxidized CaMKII causes cardiac sinus node dysfunction in mice. *J Clin Invest.* 2011;121(8):3277-3288.
75. Kikuchi K, McDonald AD, Sasano T, Donahue JK. Targeted modification of atrial electrophysiology by homogeneous transmural atrial gene transfer. *Circulation.* 2005;111(3):264-270.
76. Luker KE, Schultz T, Romine J, Leib DA, Luker GD. Transgenic reporter mouse for bioluminescence imaging of herpes simplex virus 1 infection in living mice. *Virology.* 2006;347(2):286-295.
77. Roura S, Galvez-Monton C, Bayes-Genis A. Bioluminescence imaging: a shining future for cardiac regeneration. *J Cell Mol Med.* 2013;17(6):693-703.
78. Hu YF, Dawkins JF, Cho HC, Marban E, Cingolani E. Biological pacemaker created by minimally invasive somatic reprogramming in pigs with complete heart block. *Sci Transl Med.* 2014;6(245):245ra294.
79. Schek RM, Hollister SJ, Krebsbach PH. Delivery and protection of adenoviruses using biocompatible hydrogels for localized gene therapy. *Mol Ther.* 2004;9(1):130-138.
80. Shanks N, Greek R, Greek J. Are animal models predictive for humans? *Philos Ethics Humanit Med.* 2009;4:2.
81. Brandenburger M, Wenzel J, Bogdan R, Richardt D, Nguemo F, Reppel M, Hescheler J, Terlau H, Dendorfer A. Organotypic slice culture from human adult ventricular myocardium. *Cardiovasc Res.* 2012;93(1):50-59.
82. Habeler W, Peschanski M, Monville C. Organotypic heart slices for cell transplantation and physiological studies. *Organogenesis.* 2009;5(2):62-66.
83. Camelliti P, Al-Saud SA, Smolenski RT, Al-Ayoubi S, Bussek A, Wettwer E, Banner NR, Bowles CT, Yacoub MH, Terracciano CM. Adult human heart slices are a multicellular system suitable for electrophysiological and pharmacological studies. *J Mol Cell Cardiol.* 2011;51(3):390-398.
84. Stanger BZ, Datar R, Murtaugh LC, Melton DA. Direct regulation of intestinal fate by Notch. *Proc Natl Acad Sci U S A.* 2005;102(35):12443-12448.
85. Murtaugh LC, Stanger BZ, Kwan KM, Melton DA. Notch signaling controls multiple steps of pancreatic differentiation. *Proc Natl Acad Sci U S A.* 2003;100(25):14920-14925.

86. Madisen L, Zwingman TA, Sunkin SM, Oh SW, Zariwala HA, Gu H, Ng LL, Palmiter RD, Hawrylycz MJ, Jones AR, Lein ES, Zeng H. A robust and high-throughput Cre reporting and characterization system for the whole mouse brain. *Nat Neurosci.* 2010;13(1):133-140.

87. Laughner JI, Ng FS, Sulkin MS, Arthur RM, Efimov IR. Processing and analysis of cardiac optical mapping data obtained with potentiometric dyes. *Am J Physiol Heart Circ Physiol.* 2012;303(7):H753-765.

88. Boukens BJ, Hoogendijk MG, Verkerk AO, Linnenbank A, van Dam P, Remme CA, Fiolet JW, Opthof T, Christoffels VM, Coronel R. Early repolarization in mice causes overestimation of ventricular activation time by the QRS duration. *Cardiovasc Res.* 2013;97(1):182-191.